THE VAPORIZATION AND PHYSICAL PROPERTIES OF CERTAIN REFRACTORIES

PART I. TECHNIQUES AND PRELIMINARY STUDIES

A. A. Hasapis
M. B. Panish
C. Rosen

Avco Corporation

OCTOBER 1960

WRIGHT AIR DEVELOPMENT DIVISION
AIR RESEARCH AND DEVELOPMENT COMMAND
UNITED STATES AIR FORCE
WRIGHT-PATTERSON AIR FORCE BASE, OHIO

FOREWORD

This report was prepared by Avco Research and Advanced Development Division under USAF Contract No. AF 33(616)-6840. The contract was initiated under ARPA Order 24-59, Task 6, Project No. 4776, "Material Thermal Properties"; and Project No. 7360, "Materials Analysis and Evaluation Techniques", Task No. 73603, "Heat Transfer and Thermodynamics". The work was administered under the direction of the Materials Central, Directorate of Advanced Systems Technology, Wright Air Development Division, with Mr. P. W. Dimiduk acting as project engineer.

This report covers work conducted from 1 October 1959 to 31 May 1960.

ABSTRACT

Simple effusion studies of the vaporization of rhodium, iridium, and osmium have been undertaken by the Knudsen effusion technique. The rate of effusion was determined by condensing the molecular beam on a target. Rhodium was studied from 2051 to 2205 °K. In this temperature range, its heat of vaporization was found to be 129 Kcal/mole. Iridium was studied from 2100 to 2600 °K. In this range, its tentative heat of vaporization is 155 ± 5 Kcal/mole. It was noted that some interaction between the iridium, the thoria liner, and the tungsten outer liner of the effusion cell may have occurred. No data were obtained for the vaporization of osmium because of extensive interaction between the thoria liner and the tungsten outer liner of the effusion cell.

Mass spectrometric studies have been made of the vaporization of thoria from tungsten effusion cells. Interactions between thoria and tungsten at elevated temperatures were noted. Tentative data on the vaporization of thoria to ThO and ThO_2 were obtained and are presented.

Mass spectrometric studies of the vaporization of Al_2O_3 in contact with tungsten have been made in conjunction with compatability studies of tungsten and Al_2O_3. Data are given for the vaporization of Al_2O_3 in tungsten to yield Al, AlO, Al_2O, and WO_2. More information will be needed before thermodynamic calculations can be made for this system.

The continuously monitored effusion apparatus, the null-point effusion apparatus, the oscillating cup viscometer, and the sessile drop equipment have been constructed and calibrated.

The viscosity of fused silica has been determined at temperatures up to 2560 °C where $\eta = 10^{4.44}$ poises. The viscosity of alumina has been measured using an iridium crucible up to 2200 °C and determined to be approximately 13 poises.

PUBLICATION REVIEW

This report has been reviewed and is approved.

FOR THE COMMANDER:

J. I. WITTEBORT
Chief, Thermophysics Branch
Physics Laboratory
Materials Central

TABLE OF CONTENTS

LIST OF FIGURES

WADD TR 60-463 Pt I

I. VAPORIZATION STUDIES

A. EXPERIMENTAL TECHNIQUES

There are only a limited number of vapor pressure measurement methods which are applicable, with a reasonable assurance of success, to high temperature materials. At very low pressures, the methods most used and most practical have been based either upon Langmuir rate of evaporation measurements or Knudsen effusion techniques. The Knudsen effusion technique is particularly useful and may be combined with mass spectrometric studies to yield information regarding partial vapor pressures of species in equilibrium with a condensed phase.

In the latter method the material to be studied is placed in an effusion cell. The cell and the space surrounding it are then evacuated. The effusion cell is, in the ideal case, an inert container with a small orifice. From the kinetic theory of gases, the number of moles, n, of a gas passing out of the container per second through an ideal orifice of area, a, (cm^2) at temperature T (°K) and pressure p (dynes/cm^2) is

$$n = pa(2\pi MRT)^{-1/2} \tag{1}$$

where M is the molecular weight of the gas molecule or atom and R is the gas constant.

If we place a collimator in a plane parallel to the plane of the orifice, with the collimator center coaxial with the orifice center, the fraction, f, of the molecules which effuse from a small ideal orifice and pass through the circular collimator is

$$f = \frac{D^2}{D^2 + 4L^2} \tag{2}$$

where D is the collimator diameter and L is the distance from the orifice to the collimator.

Thus, with a knife-edged orifice in the effusion cell and a collimator, the number of moles which pass through the collimator per second, after effusing from the orifice, is

$$n = \frac{pa D^2 (2\pi MRT)^{-1/2}}{D^2 + 4L^2} \tag{3}$$

-1-

or

$$p = \frac{n(D^2 + 4L^2)(2\pi RMT)^{1/2}}{aD^2} \tag{3a}$$

The pressure p is then assumed to be equal to the true pressure if

$$\frac{a}{\alpha A} << 1 \tag{4}$$

where A is the surface area of the evaporating material and α is its accommodation coefficient. For metals, the accommodation coefficient is generally unity.

1. Simple Effusion Studies

Studies of the vaporization of several materials were undertaken under this contract using a Knudsen effusion technique in which the rate of effusion of the material from the effusion cell was found by determining the weight of condensate collected on a cold surface. This particular method has been designated as the simple effusion technique.

The effusion cells used in these studies are shown in Figures 1 and 2, and a schematic diagram of the containing assembly and auxiliary apparatus is shown in Figure 3.

The cell is constructed from two pieces of tungsten and contains a thoria liner. A single radiation shield surrounds the cell except where it is necessary to have openings for supports, electrical leads, the effusion hole, and for viewing the blackbody hole. The cell is heated by electron bombardment from two filaments which loop around its upper and lower halves. Each half of the cell is heated independently from the other. The cell temperature is measured with a micro-optical pyrometer from light collected from the blackbody hole in the lower part of the cell. The optical system and pyrometer are calibrated by measuring the brightness temperature of a tungsten ribbon lamp which had been calibrated by the National Bureau of Standards. The cell halves are held at the same temperature by manual regulation of the power to the two filaments, based on temperature checks of the cell halves through the observation port shown in Figure 3. The cell temperature is thus maintained at T ± 5°C and the two halves are held within 5° to 10°C of each other during a run. The target assembly shown in Figure 3 holds twelve copper target holders in a liquid nitrogen cooled magazine. A target holder, with enclosed platinum or copper target, is shown in Figure 4. Before insertion into the target holders, the targets were chemically cleaned, dried, and where direct weighing was to be done, weighed on a Sartorius microbalance to ± 5 micrograms.

WADD TR 60-463 Pt I

$\frac{1"}{16}$ — THO$_2$ INNER LINER

$\frac{3"}{16}$

$\frac{3"}{16}$

TUNGSTEN
CONTAINER

BLACK BODY HOLE

EFFUSION CELL SUPPORT ROD
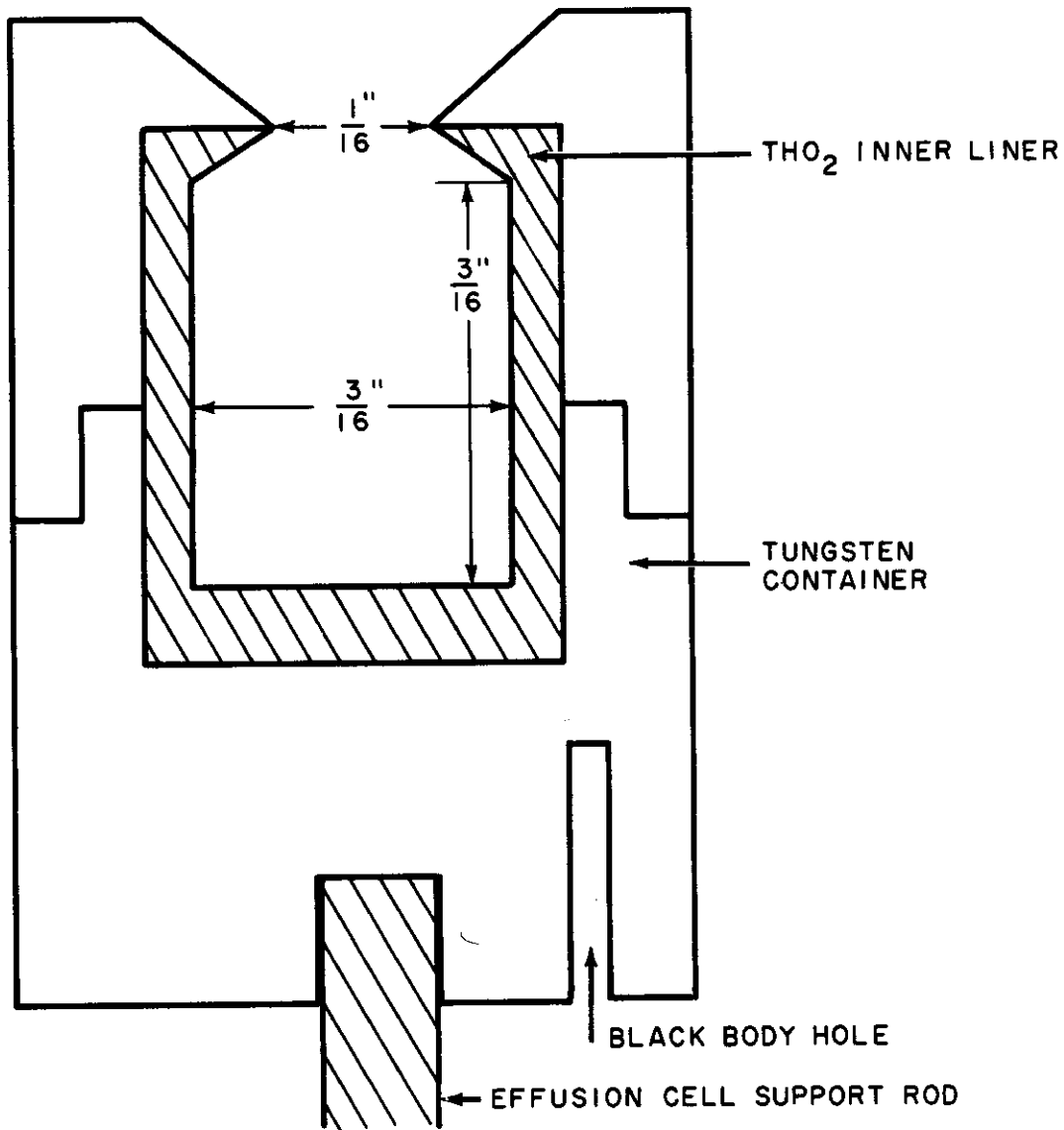
Figure 1 EFFUSION CELL NO. 1

WADD TR 60-463 PtI

-3-
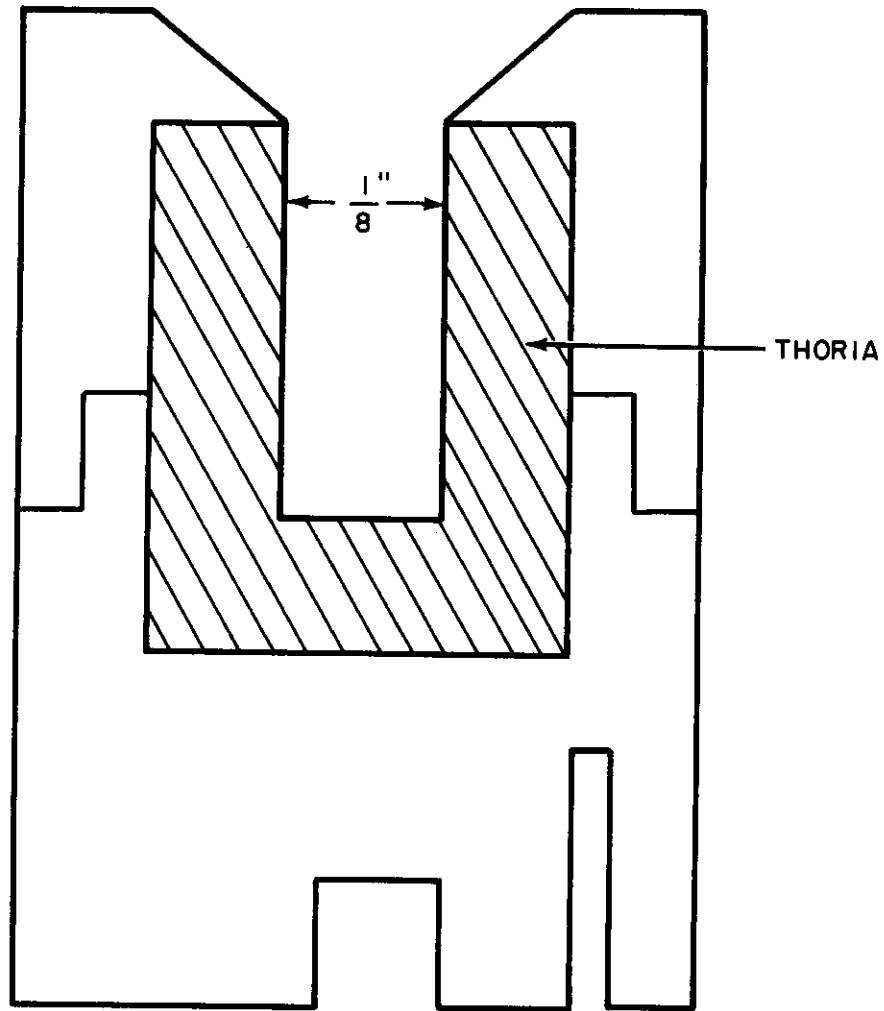
Figure 2 EFFUSION CELL NO. 2

WADD TR 60-463 PtI

-4-

DEWAR FOR LIQUID NITROGEN

KOVAR SEAL

COPPER MAGAZINE

TARGET HOLDERS

TARGET EJECTOR

USED TARGET STORAGE

COLLIMATOR

SHUTTER

WATER COOLED BAFFLES

TO IONIZATION GAUGE

TO PUMPING SYSTEM

VIEWING PORT

EFFUSION CELL

FILAMENT SUPPORTS

RADIATION SHIELD

INSULATED SUPPORTS

HEATER CURRENT & HIGH VOLTAGE LEADS

SHUTTER

TO OPTICAL PYROMETER
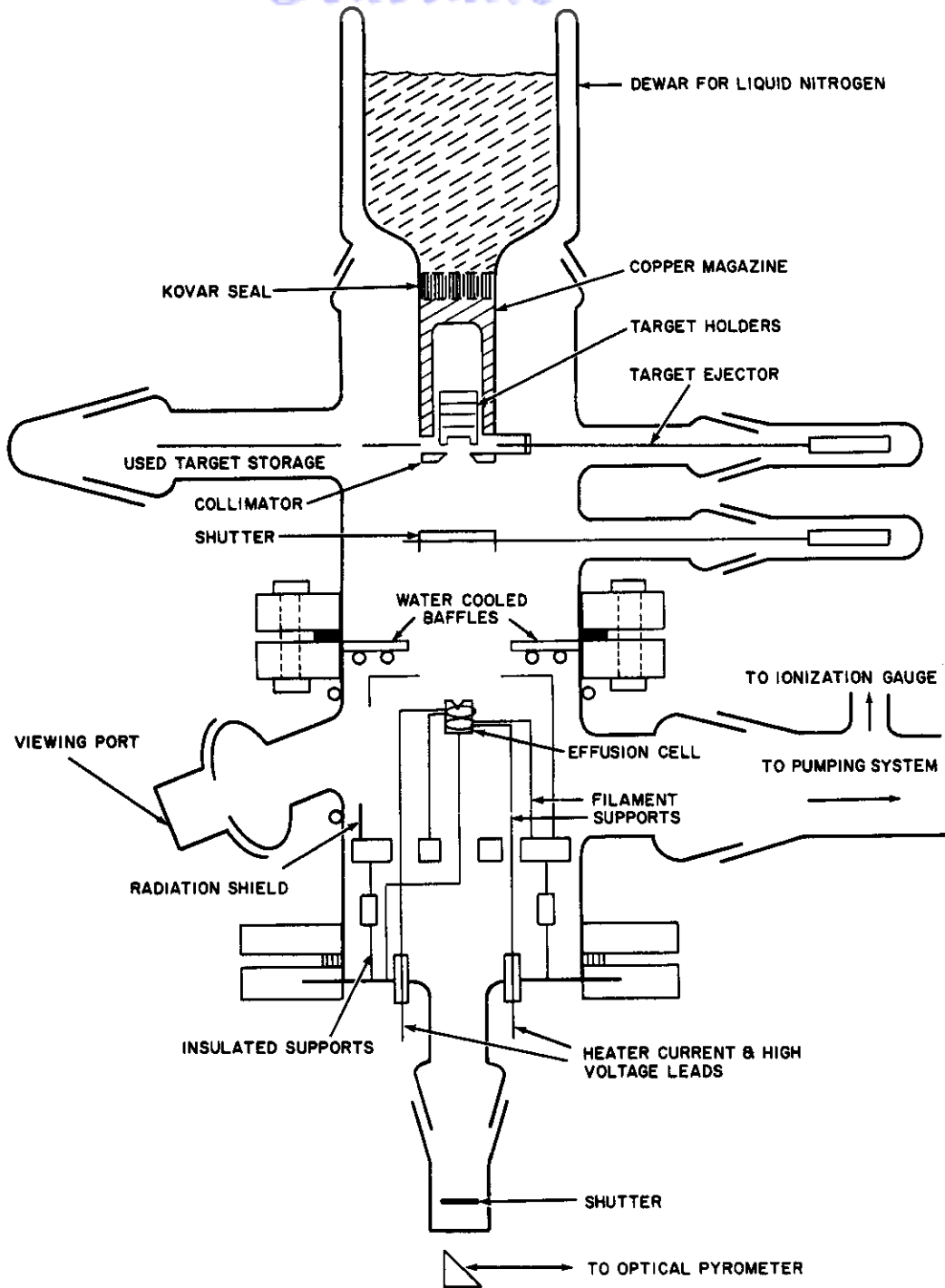
Figure 3 SCHEMATIC DIAGRAM OF THE SIMPLE EFFUSION APPARATUS

WADD TR 60-463 PtI

-5-

SECTION AA

TUNGSTEN
SPRING

TARGET

A   A

TARGET HOLDER

Figure 4 TARGET HOLDER DETAILS

WADD TR 60-463 PtI

The molecular beam from the effusion cell was interrupted with a magnetically operated shutter. After a target was exposed to the beam for a specific amount of time, the shutter was closed and the target ejected magnetically into the storage chamber.

In some of the studies radioactive tracers were used to determine the amount of material which had condensed upon the target. When such a procedure was used, the radioactivity of the target with the condensed sample was compared with that of a standard radioactive sample containing the same ratio of tracer to natural isotopes and a known total weight of the reference material. Counting was done with a standard well-type crystal counter.

2. Mass Spectrometric Studies

The mass spectrometric studies were conducted with a Bendix time-of-flight mass spectrometer. The source end of the mass spectrometer, shown in Figure 5, consists essentially of a set of grids, an entrance slit, and an elect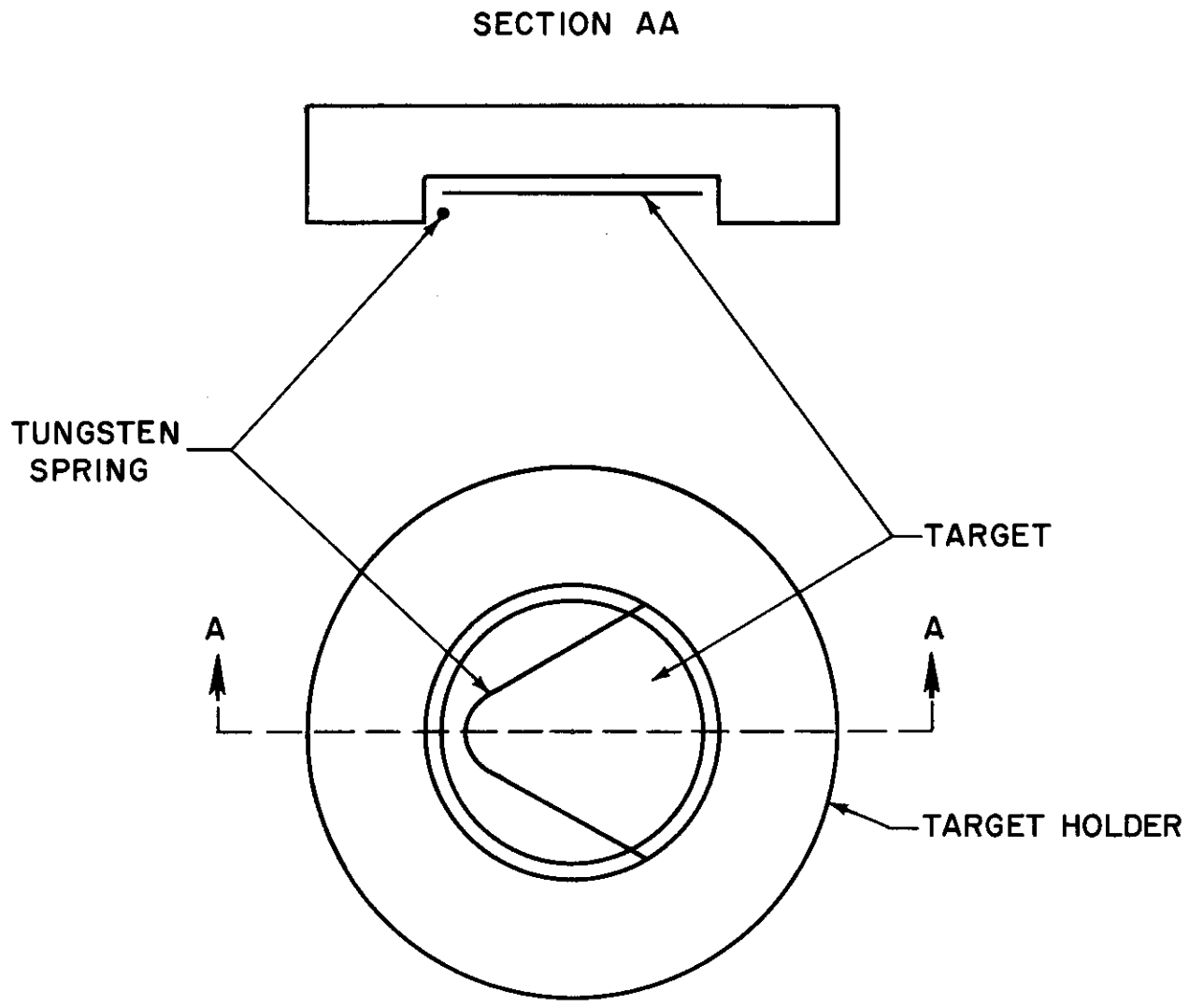ron gun. Ions formed in the ionization chamber are pulsed out down the field-free flight tube by the grids illustrated, at a repetition frequency of 10,000 cycles per second. At the end of the flight tube, the ions impinge upon a magnetic electron multiplier which functions both as the ion signal detector and amplifier. Positive ions are produced from neutral species by electron impact in the ionization chamber. The current, I_n^+, collected, is proportional to the density of neutral species of n in the ionizing region. In the case where a Knudsen cell is effusing a beam of neutral species into the ionizing region, the pressure p of a particular species within the effusion cell is proportional to $I_n^+ T$ where T is the temperature within the effusion cell in degrees Kelvin. A plot of $\log I_n^+ T$ versus $1/T$ is therefore equivalent to the $\log p$ versus $1/T$ plots ordinarily used in analyzing vapor pressure data.

The velocity with which the ions travel down flight tube is inversly proportional to the square root of the mass to charge ratio since all the ions receive the same kinetic energy from the pulsed grids. The time of flight, which is determined with the mass spectrometer, is thus directly proportional to the square root of the mass to charge ratio. Identification of species in the mass spectrometer is thus achieved by determining their time of flight. This is illustrated in Figure 6 in which $\sqrt{m/e}$ is plotted against a number proportional to the time of flight of the ions. In Figure 6, the points from $m/e = 28$ up to $m/e = 202$ were determined on the basis of known ions from nitrogen, oxygen, CO_2, and mercury. The points above mass 202 are obtained when solid WO_3 is heated in the effusion cell and the resulting molecular beam is projected into the ionization chamber of the mass spectrometer. The various tungsten oxide species have been identified from their time of flight values by extrapolation of the calibration line above mass 202.
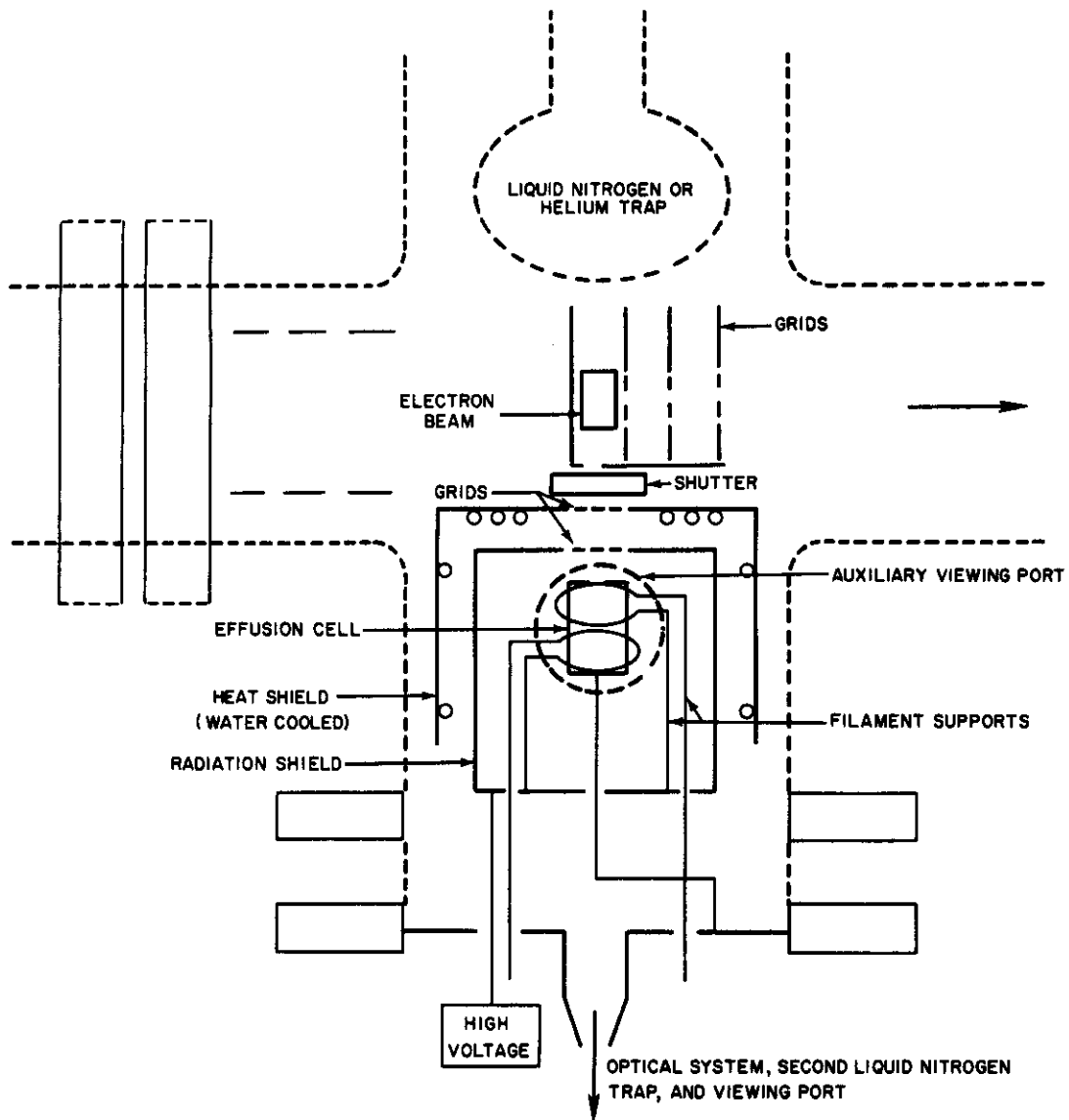
WADD TR 60-463 Pt I

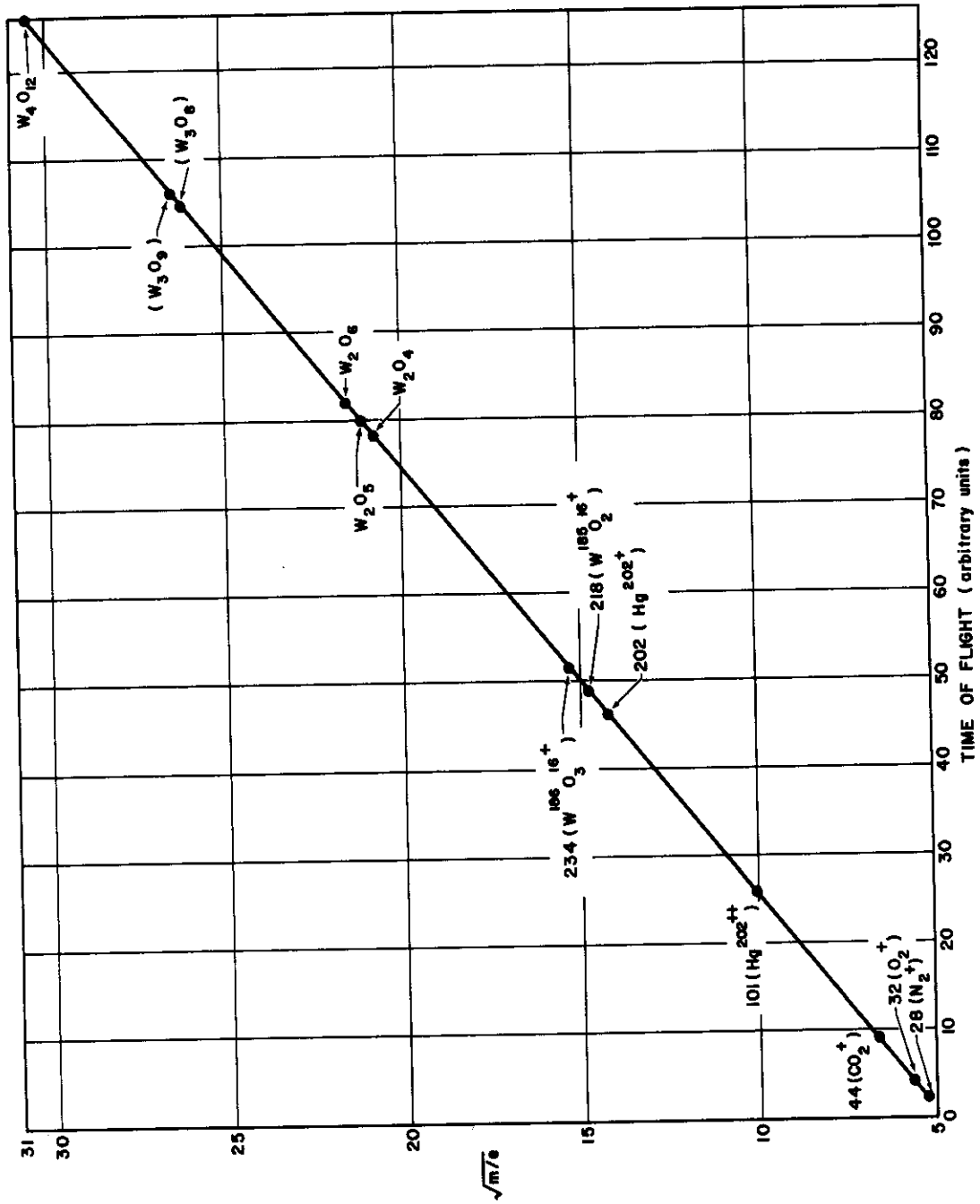Figure 5 THE EFFUSION - MASS SPECTROMETRIC SET-UP

WADD TR 60-463 PtI

-8-

Figure 6 TIME OF FLIGHT VERSUS $\sqrt{m/e}$

The unmodified instrument was intended to give maximum resolution at some sacrifice in sensitivity. For this reason, the electron beam and the entrance slit below the beam were quite narrow. An increase in sensitivity was achieved by widening both the electron beam and the entrance slit of the mass spectrometer. The source end was also modified to permit placement of the effusion cell quite close to the electron beam. With these modifications, it was possible to detect individual isotopes with an increase in sensitivity by a factor of 50 to 100. The resolution of the modified instrument permits complete separation of adjacent mass peaks to about mass 220. Greater resolution is of course desirable but not absolutely necessary. A more detailed description of the operation of the time of flight mass spectrometer has been given by Harrington.[1]

When using the Bendix mass spectrometer it is not practical to calibrate the ion current intensity in an independent experiment since the gain of the instrument may be different in each run. We have attempted to overcome this difficulty by using several internal standards during a run or by doing simple effusion studies in conjunction with the mass spectrometric studies. The details of each such procedure will be described in the following sections dealing with particular experiments.

In the Knudsen effusion studies the effusion cell is placed under the mass spectrometer entrance slit in the manner shown in Figure 5. The methods of heating, temperature measurement, and shutter operation are identical to those described earlier for the simple effusion studies. The auxiliary grids shown above the effusion cell in Figure 5 are intended to reduce noise due to electrons and ions entering the mass spectrometer from the region around the effusion cell.

3. Continuously Monitored Effusion Studies

In addition to the effusion studies already mentioned, apparatus has been constructed under this contract for the determination of Knudsen and Langmuir pressures by means of continuously monitoring the weight of the sample. Since the apparatus is a continuously monitored device:

　　a. One has to make no corrections for the fact that the sample is not at temperature during the heat up and cool down periods,

　　b. Anomalous values due to surface depletion or contamination are readily detectable, and

　　c. The entire escaping beam is weighed so that beam scattering

---

[1]Harrington, D.B., The Time-of-Flight Mass Spectrometer, Recent Advances in Mass Spectrometry, p 249, J. D. Waldron Ed., Pergamon Press, N.Y., (1959).

WADD TR 60-463 Pt I

-10-

beyond the orifice does not influence the results, enabling experiments to be performed with high backgound pressures.

This continously monitored effusion apparatus can also be used to obtain the force of the beam of effusing molecules. With an orifice located on top of the furnace the change in weight of the crucible, on quenching the furnace temperature, is due entirely to the force of the escaping molecules.

The force of the beam is directly related to pressure while the weight loss per unit time is related to the product of pressure and square root of the molecular weight of the evaporating molecules. Thus, with the present apparatus we obtain both the pressure and the average molecular weight from one experiment.

The weighing device that will be used for these experiments is shown in Figures 7 and 8.

The effusion cell, centrally located inside of a tungsten resistance furnace, (Fig. 10), is suspended from one arm of a "Sartorius Semi-Micro" analytical balance. Also rigidly attached to this arm of the balance is an Alnico V Magnet which is coaxial with a solenoid. The weight of the sample is determined by calibrating the force of repulsion between the solenoid and the magnet in terms of current going through the solenoid. The current is supplied from a battery of dry cells and is determined by measuring the voltage drop across a resistance in series with it, and the current is altered by varying resistance in series with the dry cells and the solenoid (Fig. 9).

The force between the solenoid and the magnet is directly proportional to the current only for a fixed geometry, (in our case the null position of the balance). The null position of the system is sensed by a linear variable differential transformer (LVDT) whose core is rigidly attached to the balance beam. As the beam is displaced from its null position due to a change in weight, an error voltage with magnitude proportional to the displacement and phase related to the direction of displacement is produced at the secondaries of the LVDT. This error voltage is amplified and drives a two phase a-c motor (servo-motor) which varies the current in the soenoid by turning a helical potentiometer in such a manner as to bring the beam back to its null position.

Also developed under this contract is a null point torsion effusion apparatus.

Torsion effusion apparatuses have been described in the literature and offer an extremely rapid and relatively accurate method of determining vapor pressures. However, they have several major drawbacks:

WADD TR 60-463 Pt I
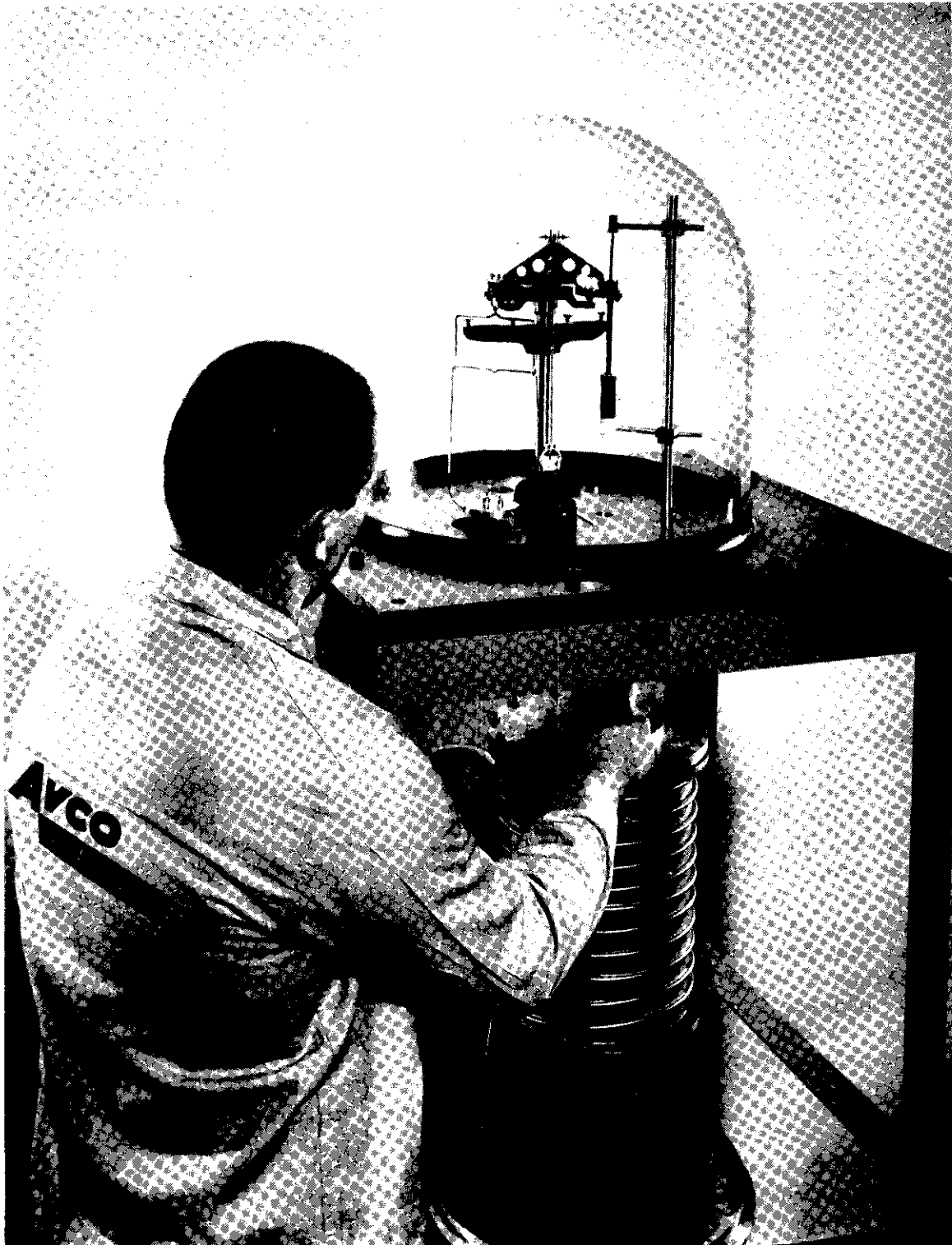
Figure 7 WEIGHING DEVICE

WADD TR 60-463 PtI

-12-

ANALYTICAL
BALANCE BEAM

BELL JAR

DIFFERENTIAL
TRANSFORMER

TRANSDUCER CORE
RIGIDLY MOUNTED
TO BEAM

SOLENOID

BEAM
ARREST
MECHANISM

MAGNET

GASKET

TO FURNACE

TUBE TO PREVENT
RECONDENSATION
OF EFFUSATE

SAMPLE SUSPENSION WIRE
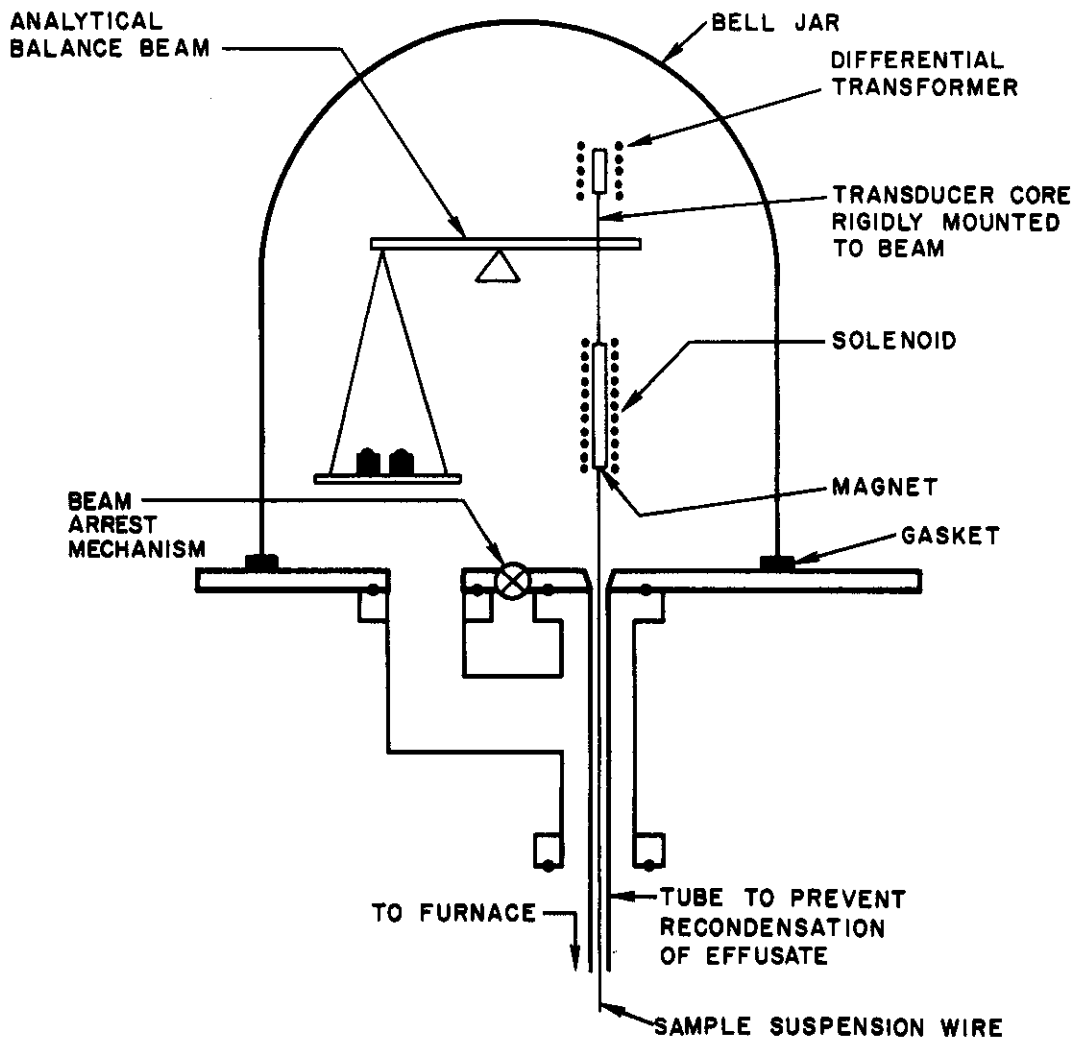
Figure 8 CONTINUOUSLY MONITORED WEIGHING DEVICE

WADD TR 60-463 PtI
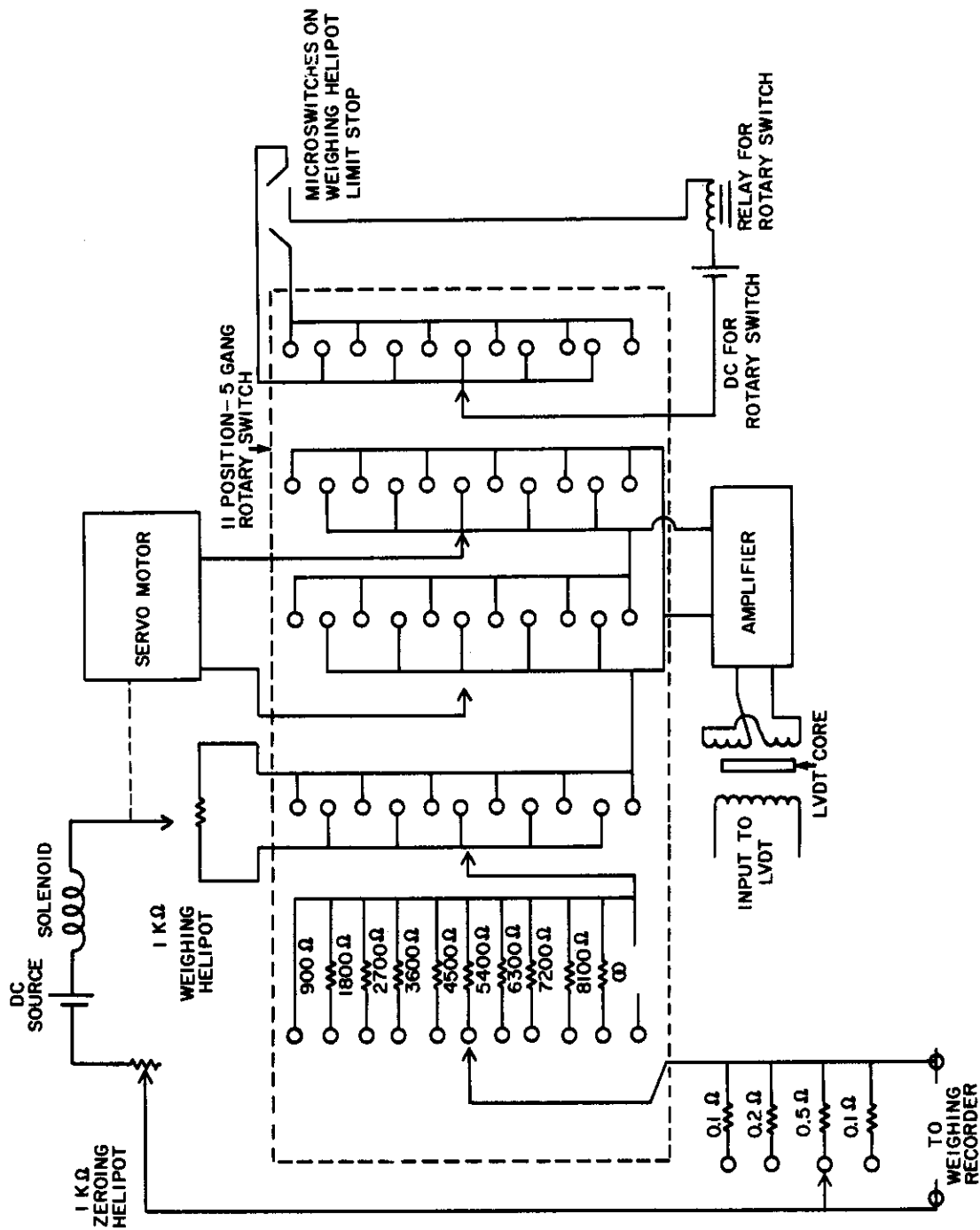
Figure 9 ELECTRICAL CIRCUIT FOR WEIGHING DEVICE

WADD TR 60-463 PtI

-14-
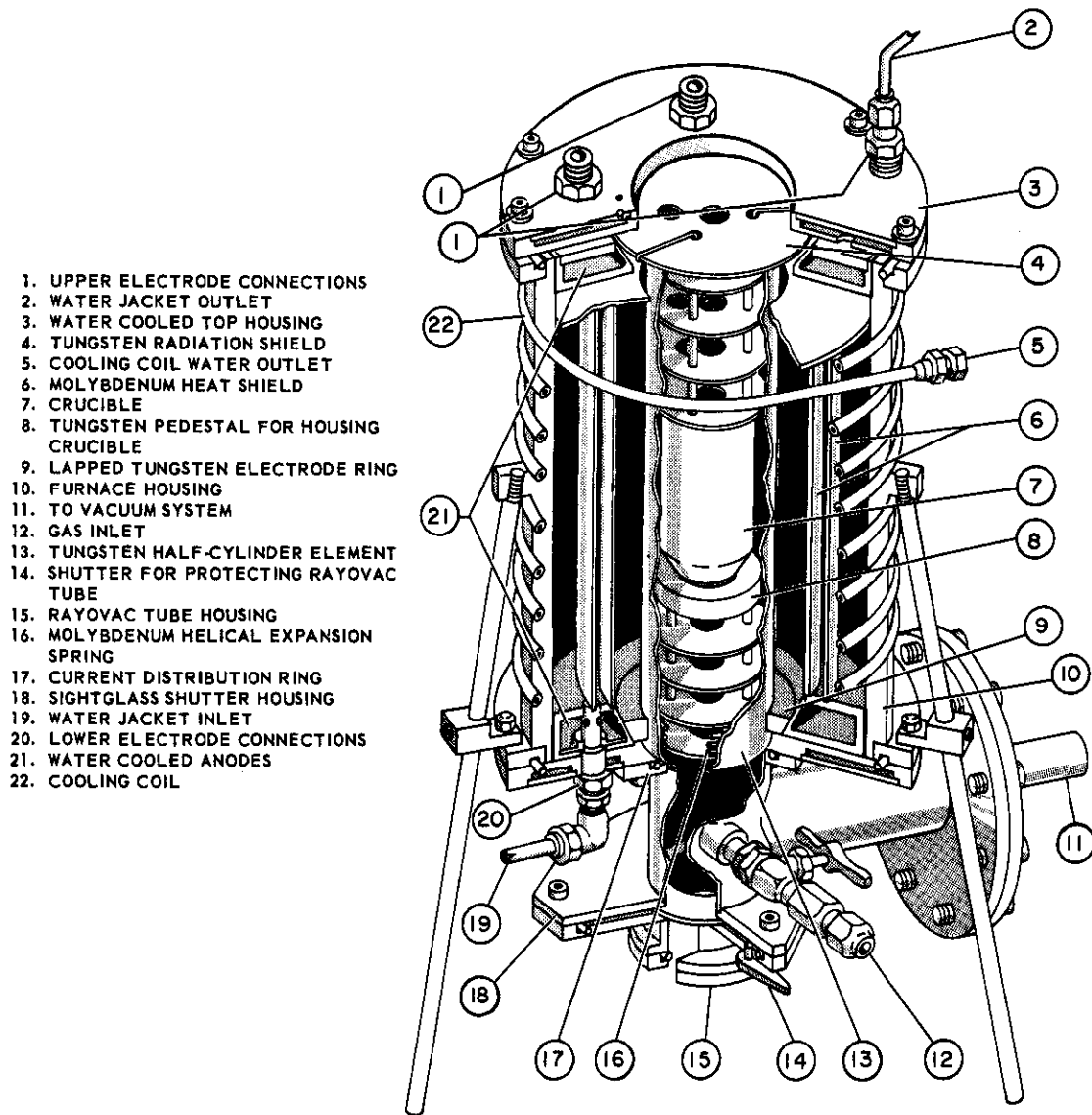
1. UPPER ELECTRODE CONNECTIONS
2. WATER JACKET OUTLET
3. WATER COOLED TOP HOUSING
4. TUNGSTEN RADIATION SHIELD
5. COOLING COIL WATER OUTLET
6. MOLYBDENUM HEAT SHIELD
7. CRUCIBLE
8. TUNGSTEN PEDESTAL FOR HOUSING CRUCIBLE
9. LAPPED TUNGSTEN ELECTRODE RING
10. FURNACE HOUSING
11. TO VACUUM SYSTEM
12. GAS INLET
13. TUNGSTEN HALF-CYLINDER ELEMENT
14. SHUTTER FOR PROTECTING RAYOVAC TUBE
15. RAYOVAC TUBE HOUSING
16. MOLYBDENUM HELICAL EXPANSION SPRING
17. CURRENT DISTRIBUTION RING
18. SIGHTGLASS SHUTTER HOUSING
19. WATER JACKET INLET
20. LOWER ELECTRODE CONNECTIONS
21. WATER COOLED ANODES
22. COOLING COIL

Figure 10 TUNGSTEN RESISTANCE FURNACE

WADD TR 60-463 PtI

-15-

a. The torsional constant of the wire is subject to change and also to hysteresis effects,

b. Only a small fraction of the possible rotation of the suspension wire is visible in most high temperature equipment, and

c. Separate torsion wires must be used for different pressures in order to stay within the given angular displacement and within a given accuracy.

These objections to the torsional method are eliminated in the present apparatus by counterbalancing with electromagnetic force the torsional force of effusion. The wire now acts only as a bearing, and its torsional constant only influences the lower limit of the sensitivity of the system. The more flexible the wire, the greater is the sensitivity. Also, a single suspension wire can now be used for all experiments since the force between the magnet and the solenoids is influenced only by the current going through the solenoids. The magnet and solenoids also act as a damping device to eliminate many of the extraneous oscillations usually present.

The apparatus is shown in Figures 11 and 12. The torsion suspension wire is connected at one end to a micrometer head, and at the other end to an aluminum rod to which is rigidly attached an Alnico V magnet. The effusion cell, centrally located inside the tungsten furnace (Fig. 10), is rigidly mounted to the aluminum rod. A mirror is cemented to the rod and can be viewed through a sight port, which allows 120 degrees of rotation. Enough current is passed through the solenoids to exactly counterbalance any torsional force on the system due to effusion. Since the force between the magnet and solenoid, for a fixed geometry, is proportional only to the current, the vapor pressure is thus proportional to the current going through the solenoids. The constants of the system are are determined by calibration with materials of known vapor pressure. (See Appendix I.)

In favorable cases, we intend to extend the use of the torsion effusion and continuously monitored weighing apparatus to the determination of phase diagrams of refractory systems.

B. MATERIALS STUDIED AND RESULTS

1. Rhodium

The vapor pressure of solid rhodium was studied by the simple effusion technique using the 1/8-inch cell illustrated in Figure 2. The data are given in Table 1 and plotted in Figure 13. In the pressure calculations, equation 3a was used. Since no radioisotope of rhodium was available,

WADD TR 60-463 Pt I

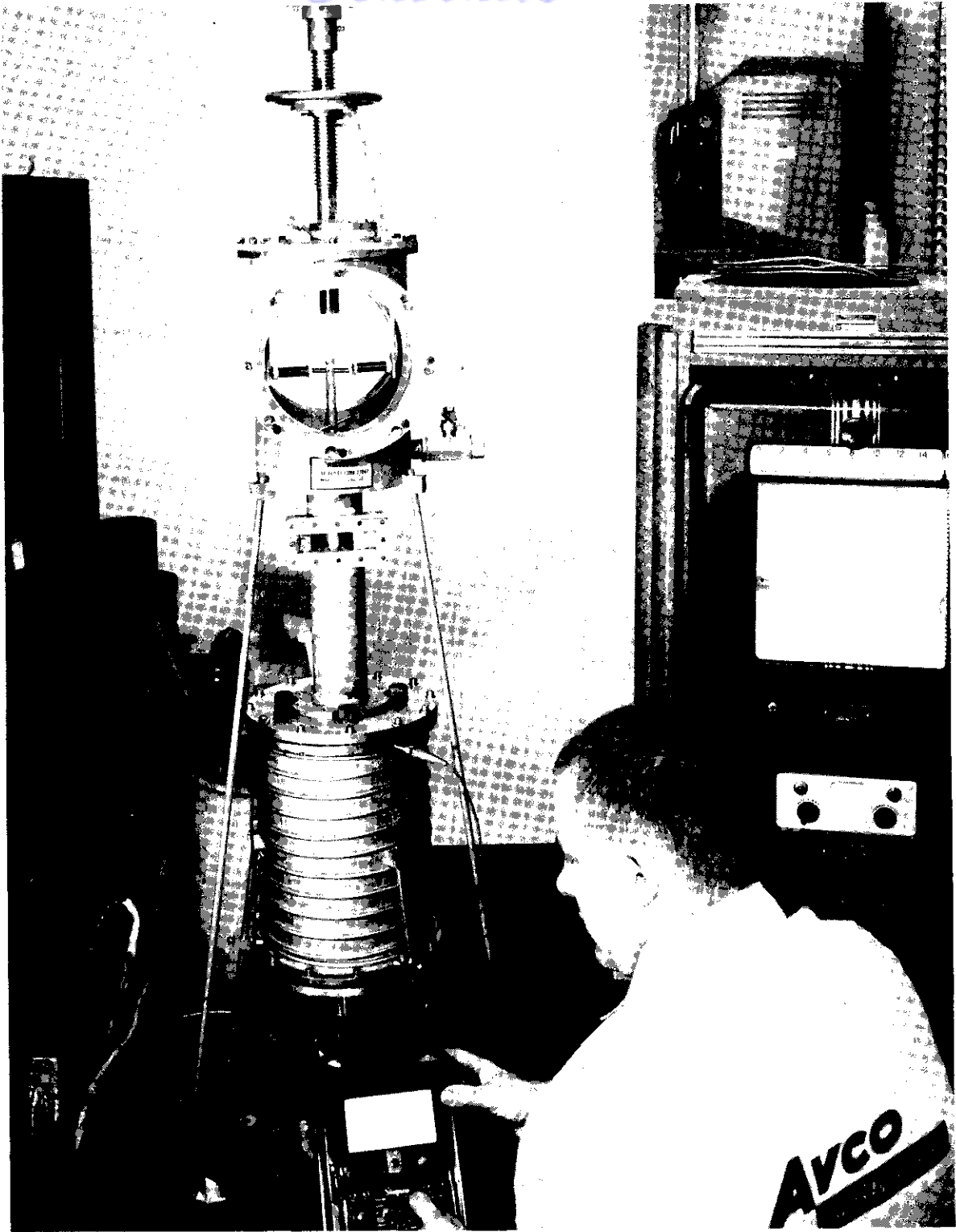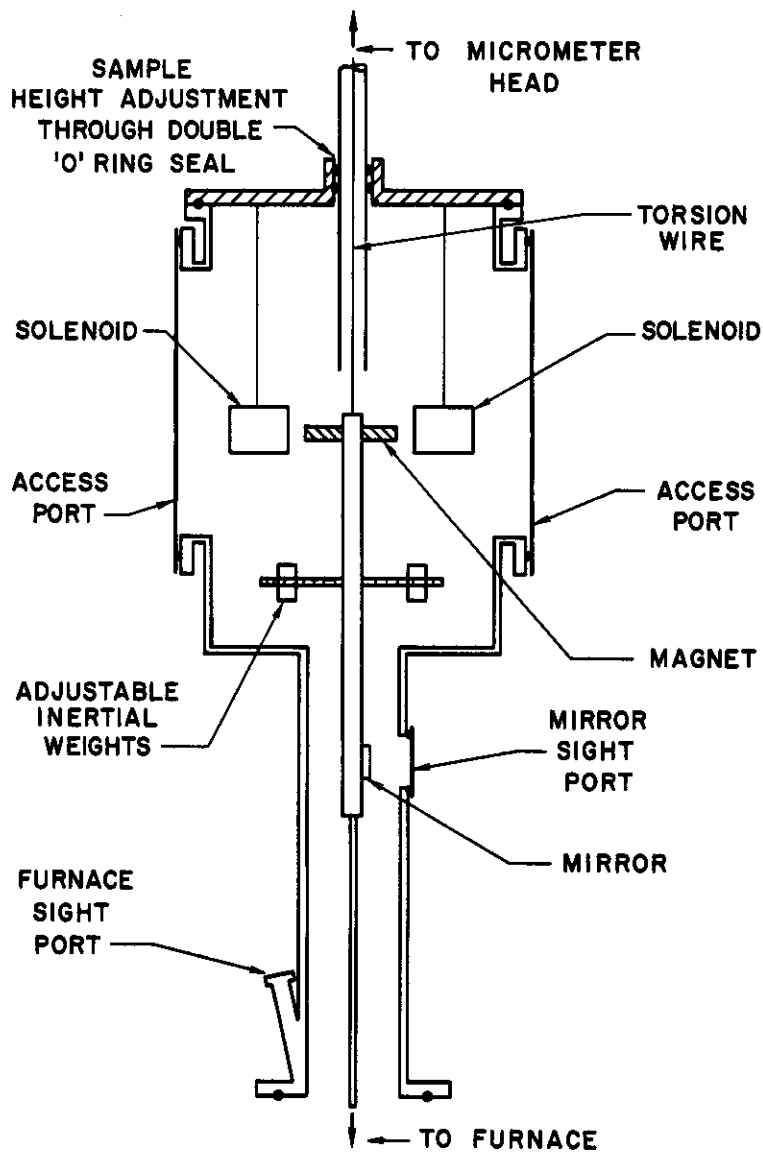Figure 11 NULL-POINT TORSION EFFUSION APPARATUS

WADD TR 60-463 PtI   -17-

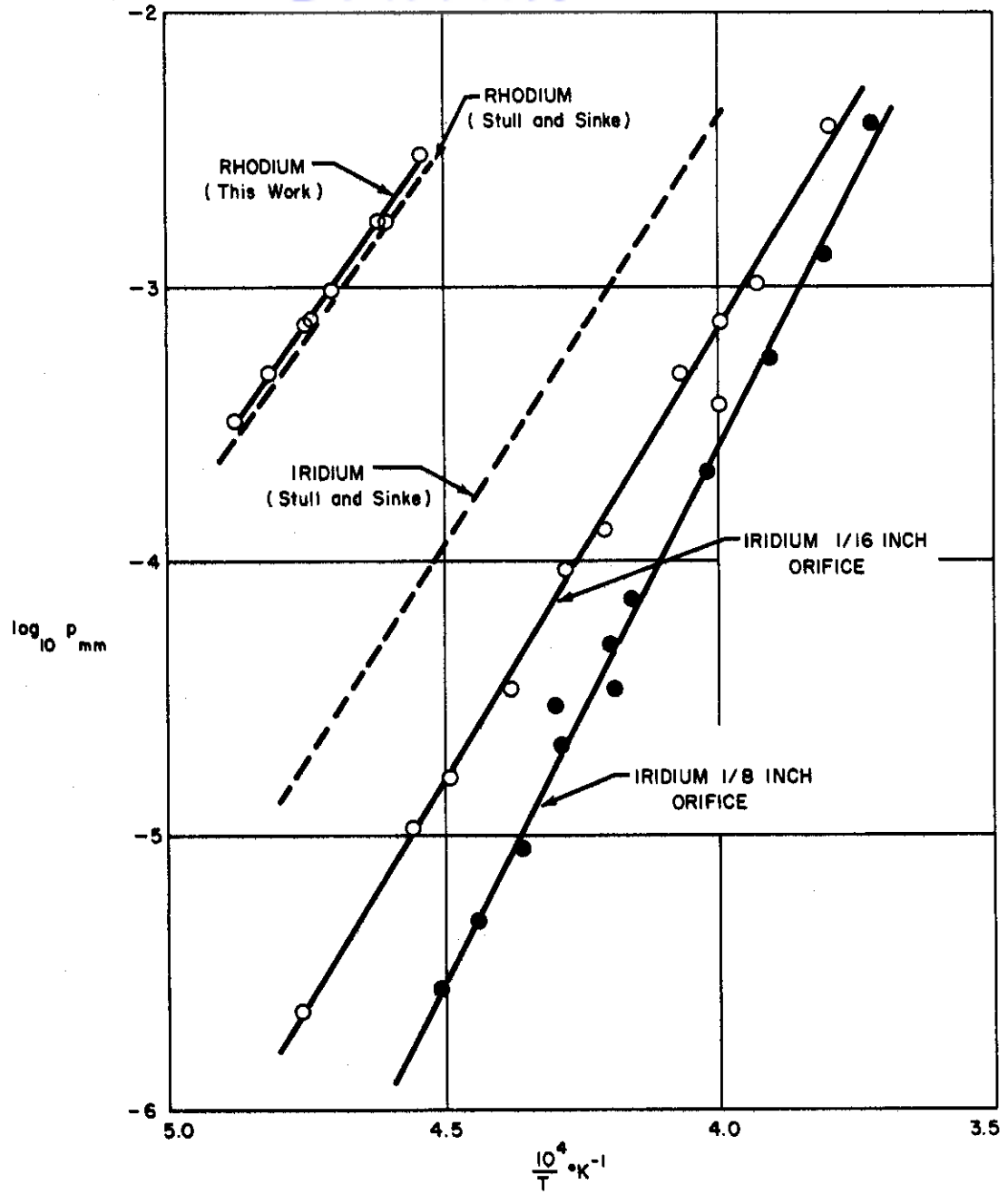Figure 12 NULL-POINT TORSION EFFUSION APPARATUS

WADD TR 60-463 PtI

-18-

Figure 13 $Log_{10}P$ VERSUS $1/T$ PLOTS FOR RHODIUM AND IRIDIUM

WADD TR 60-463 PtI

the targets were weighed to the nearest 5 micrograms on a Sartorius microbalance. It is necessary to bear in mind that a number of assumptions need to be made in interpreting the results of these experiments. It was assumed that no correction need be made for the fact that a cylindrical channel was actually used rather than a sharp-edged orifice since the sample was collected only at small angles to the axis of the cell. It was shown mass spectrometrically that the effusing rhodium species are monatomic. Another assumption, which is usually made, is that the accommodation coefficient for the collisions of the atoms on the cold target is equal to unity. The assumption is probably justified since the results of vapor pressure studies are the same with copper or platinum targets.

TABLE 1 VAPOR PRESSURE OF RHODIUM*

Run	$T°K$	$\dfrac{10^4}{T}$	Exposure Time (hrs)	Weight of Sample Collected (μgm)	$P_{(mm)}$	$\log_{10} P$
A	2051	4.88	5.17	29	3.20×10^{-4}	-3.49
B	2077	4.82	6.00	50	4.88×10^{-4}	-3.31
A	2106	4.75	1.00	13	7.50×10^{-4}	-3.13
A	2111	4.74	2.50	33	7.66×10^{-4}	-3.12
B	2130	4.70	4.00	67	9.89×10^{-4}	-3.01
A	2168	4.61	2.00	58	1.71×10^{-3}	-2.77
B	2182	4.62	2.00	57	1.70×10^{-3}	-2.76
B	2205	4.54	1.50	75	3.05×10^{-3}	-2.52

*Effusion cell orifice diameter = 1/8 inch
Run A, L (orifice to collimator distance) = 7.64 cm
Run B, L (orifice to collimator distance) = 7.7 cm
     D,   (collimator diameter) = 1.05 cm
     a,   (orifice area) = 7.94×10^{-2} cm^2
Run A, - Copper Targets
Run B, - Platinum Targets

WADD TR 60-463 Pt I

The vapor pressures obtained for solid rhodium are in good agreement with those estimated by Stull and Sinke[2] from spectroscopic data. The dotted lines in figure 13 are from Stull and Sinke's data.

From the slope of the solid line drawn through our data points, and the integrated Clausius-Clapyron equation, we find the heat of vaporization of solid rhodium to be 129 Kcal per mole over the temperature range studied. We used Stull and Sinke's estimated data for $H_T^o - H_{298}^o$ for the gas and solid, and calculated ΔH_{298} sublimation to be 133 Kcal/mole. Using Stull and Sinke's estimated heat of fusion of 5.2 Kcal/mole, we obtain a heat of vaporization of 124 Kcal/mole for liquid rhodium just above the melting pint. Reliable vapor pressure data for liquid rhodium have not yet been obtained.

2. Iridium

The vaporization of solid iridium was studied by the simple effusion technique. The effusion cells and containing assembly used in this work are identical to those shown in Figures 1 and 2. The temperature measurements, the method of heating, and the sample collection technique were all identical to those described above. The amount of material collected on the targets was determined by the use of Ir^{192} or Ir^{194} as the radioactive tracer. Absolute determination of the amount of iridium on the target was obtained by comparison of the amount of radioactivity from the iridium collected with the radioactivity from iridium in a standard sample.

Samples of iridium, containing radioactive iridium, were prepared for the effusion studies by adding about two millicuries of $Na_2 Ir Cl_6$ to about 0.7 gm $Na_2 Ir Cl_6$ from natural iridium. Iridium powder was obtained from this solution by forming the ammonium salt, drying, and thermally decomposing the residue. The standard solution was prepared by reforming the salt from a small, weighed portion of the iridium powder.

Effusion data were obtained with both effusion cells. After the experiments were completed, the following observations were made.

 a. The thoria liner became black upon heating. This is apparently an indication that the remaining thoria was somewhat depleted in oxygen. X-ray diffraction studies of the thoria assemblies showed no indication that anything but ThO_2 was present. Lattice spacings were normal.

 b. In some of the experiments, the iridium appeared to have partially fused at temperatures below the melting point.

---

[2]Stull, D. R. and G. C. Sinke, Thermodynamic Properties of the Elements, American Chemical Society, Washington, D.C. (1956).

c.   When the 1/8-inch cylindrical effusion cell (Fig. 2) was used, the iridium sintered into a button of very small effective surface area. This is in marked contrast to the behavior of the rhodium used in the previous runs. The cells and samples used in the studies of rhodium were prepared by tamping the powder around the sides of the cell. When heated and sintered, the rhodium retained its shape in the effusion cell.

From the above, it appears that there may be some degree of interaction between the iridium, the tungsten outer liner, and the thoria. (See section V.) This interaction may have been only slight when the simple effusion studies of iridium were made because of the relatively short periods of time that the cell was at very high temperatures. In the mass spectrometric studies discussed in the next section, the interaction was found to be more severe and apparently involved the tungsten outer container.

The data for the vaporization of iridium are given in Table 2 and are plotted in Figure 13. Pressures were calculated by the method described previously. The estimated values of Stull and Sinkle[2] have also been plotted in Figure 13 for comparison. Observation of the vaporization of iridium in the mass spectrometer indicates that the vapor is primarily monatomic iridium.

As expected, the vapor pressures calculated from the data obtained when the effusion cell had a relatively small orifice and a relatively large internal volume, such as the cell with the 1/16-inch orifice shown in Figure 1 , are higher than those obtained when the 1/8-inch cylinder (Fig. 2) was used. This did not occur in the studies of the vapor pressure of rhodium because of the relatively large area of rhodium surface in the 1/8-inch cell. The iridium vapor pressures obtained here are less than those estimated by Stull and Sinke.[2] Low apparent pressures would be obtained if there were interaction with the thoria and if the effusion hole were too large. This system will require further study.

From the slope of the solid line drawn through our data points for the runs with the effusion cell shown in Figure 1 and the integrated Clausius-Clapeyron equation, the heat of vaporization of solid iridium over the temperature range studied is found to be 155 ± 5 Kcal per mole. The error was estimated by picking several possible lines through the points. Until further work is done to refine them, the present data for iridium should not be considered as final.

3.   Osmium

One simple effusion experiment was performed in an attempt to study the vapor pressure of osmium. The effusion cell was identical to that with the 1/16-inch orifice shown in Figure 1. The osmium used was part

TABLE 2 VAPOR PRESSURE OF IRIDIUM

Sample No.*	Temp. °K	$\dfrac{10^4}{T}$ ($°K^{-1}$)	Exposure Time (min)	Sample Weight (μ gm)	p_{mm}	$\log_{10} p_{mm}$	Target Material
1	2100	4.76	120	0.0238	2.29×10^{-6}	-5.64	Pt
2	2196	4.56	121	0.109	1.06×10^{-5}	-4.97	Pt
3	2228	4.49	160	0.228	1.69×10^{-5}	-4.79	Cu
4	2282	4.38	80	0.228	3.43×10^{-5}	-4.46	Pt
5	2337	4.28	40	0.311	9.40×10^{-5}	-4.03	Cu
6	2375	4.21	20	0.212	1.30×10^{-4}	-3.89	Pt
7	2454	4.07	15	0.570	4.76×10^{-4}	-3.32	Pt
8	2492	4.01	12	0.710	7.45×10^{-4}	-3.13	Cu
9	2545	3.93	5	0.410	1.04×10^{-3}	-2.99	Pt
10	2630	3.80	3	0.889	3.82×10^{-3}	-2.42	Pt
11	2291	4.36			8.9×10^{-6}	-5.05	Pt
12	2338	4.29			2.18×10^{-5}	-4.66	Pt
13	2386	4.19			3.46×10^{-5}	-4.46	Pt
14	2216	4.51	100	0.107	2.74×10^{-6}	-5.56	Cu

TABLE 2 VAPOR PRESSURE OF IRIDIUM (Cont'd)

Sample No. *	Temp. °K	$\frac{10^4}{T}$ (°K^{-1})	Exposure Time (min)	Sample Weight (μgm)	P_{mm}	$\log_{10} P_{mm}$	Target Material
15	2253	4.44	50	0.091	4.8×10^{-6}	-5.32	Cu
16	2322	4.30	20	0.221	4.96×10^{-5}	-4.53	Cu
17	2380	4.20	10	0.184	5.00×10^{-5}	-4.30	Cu
18	2401	4.16	20	0.530	7.21×10^{-5}	-4.14	Cu
19	2485	4.02	20	1.640	2.07×10^{-4}	-3.68	Cu
20	2501	4.00	5	0.667	3.71×10^{-4}	-3.43	Cu
21	2558	3.91	20	3.920	5.45×10^{-4}	-3.26	Cu
22	2627	3.81	5	2.320	1.34×10^{-3}	-2.87	Cu
23	2691	3.72	5	7.130	4.09×10^{-3}	-2.39	Cu

* 1-10, a = 1.77×10^{-2} cm^2, L = 7.70 cm, D = 1.10 cm
11-13, a = 7.94×10^{-2} cm^2, L = 7.70 cm, D = 1.10 cm
14-23, a = 7.94×10^{-2} cm^2, L = 7.64 cm, D = 1.05 cm

WADD TR 60-463 Pt I

of a "standard irradiation unit" of osmium supplied by the Oak Ridge National Laboratory. Standard solutions were prepared by dissolving a weighed amount of the material in a few drops of perchloric acid and then diluting the solution with water.

The specific activity of the osmium sample was quite low compared to that of the iridium used in the latter's vaporization studies. The vapor pressure of osmium is lower than that of iridium. It was therefore necessary to hold the effusion cell at high temperature (2300° C) for extended periods of time (several hours) in order to get a significant effused sample on the target. When this was done, the thoria effusion cell was found to have reacted extensively with the tungsten liner and the run was discontinued. We have therefore reported no data for osmium. In future studies of osmium we will use an iridium outer liner to eliminate the interaction problem.

4. ThO_2

For the studies of the vaporization of thoria by mass spectrometer techniques, effusion cells identical to those shown in Figures 1 and 2 were used. A small quantity of iridium metal was inserted into each effusion cell before the experiment was begun. The iridium was intended to serve as an internal standard.

At effusion cell temperatures near 2500° K and higher, it was possible to observe the appearance of several positive ion peaks which could be turned on or off by opening and closing the shutter above the effusion cell. The use of the shutter helped, in this manner, to differentiate those peaks which were due to species effusing into the ionization chamber from residual background peaks from other sources. These ions arrived at the mass spectrometer detector at flight times which corresponded to m/e values of 191(Ir), 193(Ir), 248(ThO), and 264(ThO_2). A slow steady leak of xenon was introduced into the system to provide several calibration points at m/e values of 129(Xe), 131(Xe), 132(Xe), 134(Xe), and 136(Xe).

The iridium and xenon were used to provide internal standards during a run. The xenon provided calibration peaks whose height fluctuated with the gain of the instrument. At each temperature a plot of the ion current intensity for each ion was obtained by scanning the mass unit range of 125 to 300 in about 20 seconds. Since all the ion peak heights occasionally fluctuate with gain in the instrument, the data were finally tabulated with all peak heights (ion currents) relative to those of xenon. The tabulated data are therefore independent of all gain fluctuations except those which may have occurred during the scan. It is assumed that these are negligible. The iridium metal within the thoria effusion cell was used to provide data on the absolute pressure of the species vaporizing from the thoria.
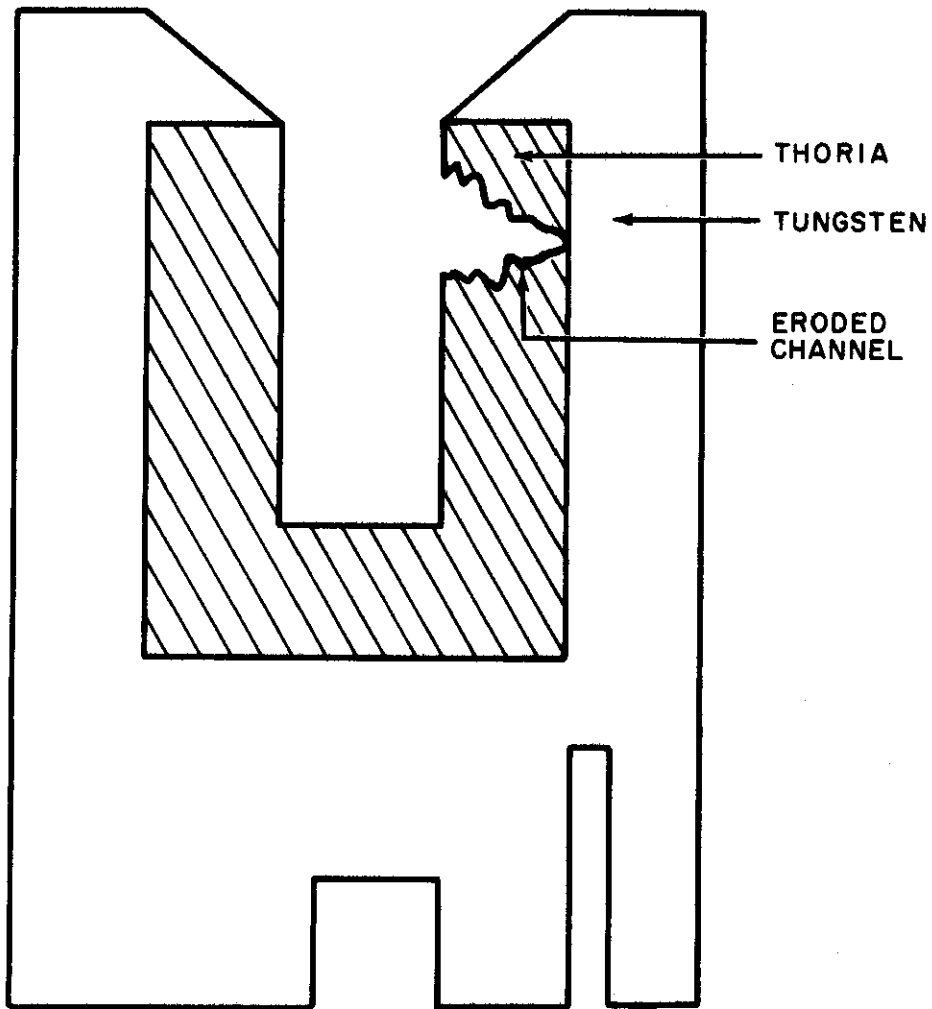
WADD TR 60-463 Pt I

THORIA

TUNGSTEN

ERODED
CHANNEL

Figure 14 THE EROSION OF A THORIA LINER IN A TUNGSTEN CONTAINER
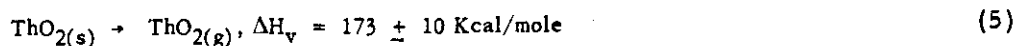
WADD TR 60-463 PtI

Several experiments were performed. First an effusion cell identical to the 1/8-inch cylinder shown in Figure 2 was used. The experiment consisted essentially of holding the crucible at each desired temperature for several minutes while a scan of the spectrum was made. The crucible was not held at the high temperatures for a prolonged period of time. During the run, the thoria cell turned black as it did in the simple effusion studies. No other obvious interaction between the tungsten, iridium, and thoria was noted.

In several experiments subsequent to those discussed above, the effusion cell with the 1/16-inch orifice shown in Figure 1 was used in an attempt to discover what effect a smaller effusion orifice would have upon the experimental results. It was noted during these experiments that the pressure of ThO_2 and ThO increased much more rapidly with temperature than it did when the other effusion cell was used, and that the iridium within the cell melted at temperatures below the melting point of pure iridium. The thoria liner itself showed extensive attack on the inside, that is, on the side not in contact with tungsten.

In order to study the interaction between tungsten and thoria in more detail, one of the thoria cells of the type shown in Figure 2 (1/8-inch) was heated at 2350° to 2400° C for several hours. After an induction period of about one-half hour, the ThO^+ and ThO_2^+ ion currents increased very markedly. No quantitative measurements were made. The cell was then inspected visually and erosion of the thoria in the manner shown in Figures 14 and 15 was found. The photograph (Fig. 15) shows a section of the crucible including a cross section of the eroded channel.

In Table 3, we have summarized the data obtained for the vaporization of ThO_2 when we used the experimental set-up shown in Figure 2 (1/8-inch). In this table, all ion current values (I^+) are taken relative to a set of references obtained from peaks due to the steady xenon leak into the system. The individual I^+ values were determined from the peak heights in plots obtained from the analog system of the mass spectrometer. The data are plotted in Figure 16. No data for effusing O or O_2 were obtained because of interference from residual background in the instrument.

The ΔH value for the reaction

$$ThO_{2(s)} \rightarrow ThO_{2(g)}, \Delta H_v = 173 \pm 10 \text{ Kcal/mole} \tag{5}$$

over the temperature range studied, was obtained from the slope of the

$\log I^+ T$ versus $\dfrac{1}{T}$ plot in the usual manner.

WADD TR 60-463 Pt I

Figure 15 PHOTOGRAPH OF EROSION OF THORIA LINER IN A TUNGSTEN
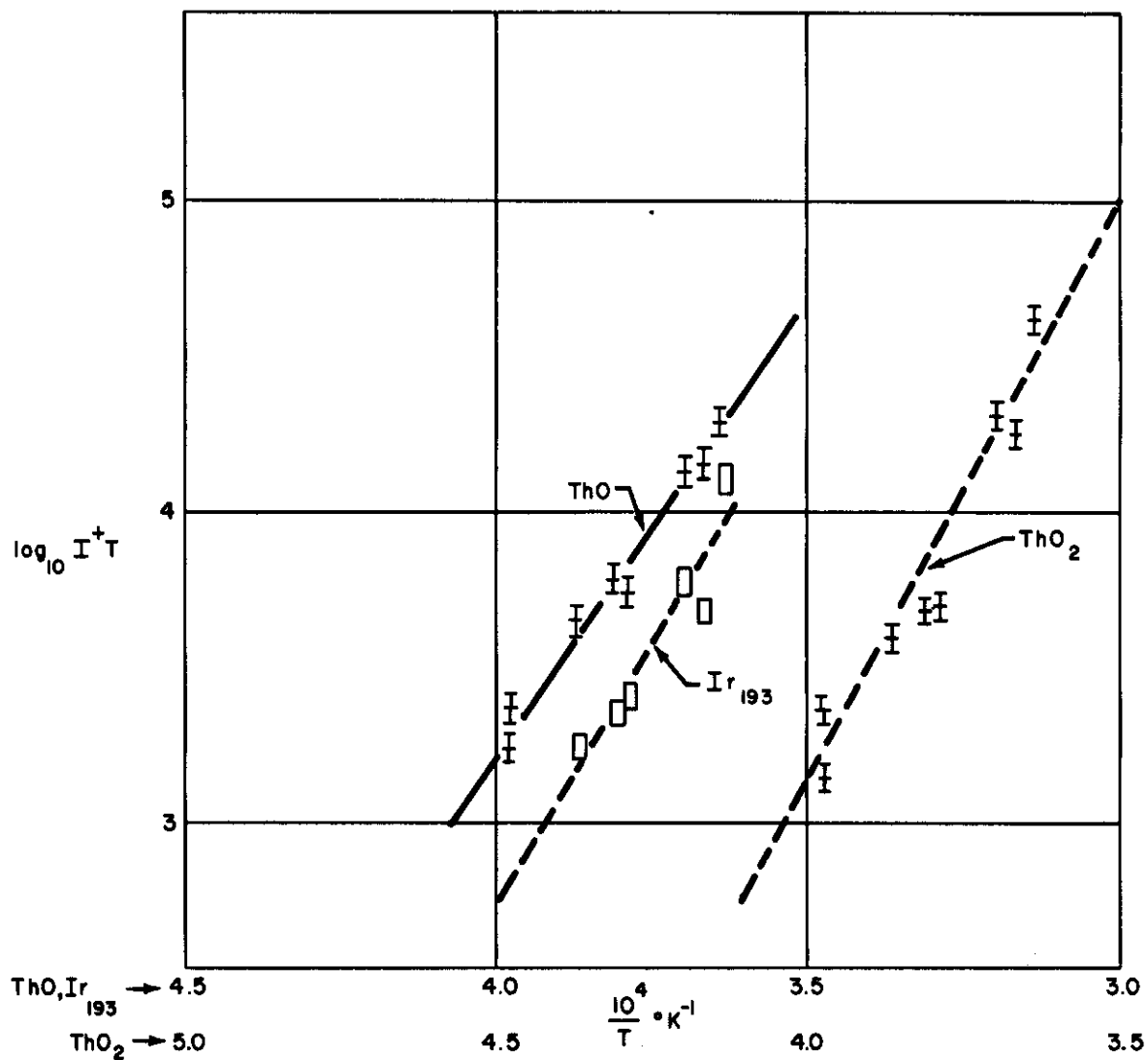CONTAINER

WADD TR 60-463 PtI

Figure 16 THE VAPORIZATION OF THORIA

-29-

TABLE 3 VAPORIZATION OF THORIA*

T °K	$\dfrac{10^4}{T °K}$	ThO I_{248}^+	ThO$_2$ I_{264}^+	Ir I_{193}^+	ThO $\log I_{248}^+ T$	ThO$_2$ $\log I_{264}^+ T$	Ir $\log I_{193}^+ T$
2513	3.98	0.92	0.92	---	3.36	3.36	---
2513	3.98	0.72	0.55	---	3.25	3.14	---
2586	3.87	1.72	1.95	≈ 0.69	3.65	3.70	≈ 3.25
2628	3.81	2.30	2.24	0.86	3.78	3.76	3.36
2638	3.79	2.06	2.35	0.97	3.74	3.79	3.41
2705	3.70	5.00	7.60	2.17	4.13	4.31	3.77
2728	3.67	5.20	6.60	1.72	4.15	4.26	3.68
2748	3.64	6.96	14.8	4.56	4.28	4.61	4.10

*All I^+ values are taken relative to $\Sigma X_e^+ = 10$

The reactions

$$ThO_{2(s)} \rightarrow ThO_{(g)} + O_{(g)} \tag{6}$$

and

$$ThO_{2(g)} \rightarrow ThO_{(g)} + O_{(g)} \tag{7}$$

are also possible.   The equilibrium constants for these reactions are for reaction (6)

$$K_p'' = (P_{ThO}) (P_O) = (P_{ThO})^2 \tag{8}$$

which is proportional to $(I_{ThO}^+ T)^2 = K_{eq}^{**}$

WADD TR 60-463 Pt I

and for reaction (7)

$$K_p''' = \frac{(P_{ThO})(P_O)}{(P_{ThO_2})} = \frac{(P_{ThO})^2}{(P_{ThO_2})} \tag{9}$$

which is proportional to

$$\frac{(I_{ThO}^+ T)^2}{(I_{ThO_2}^+ T)} = K_{eq}^{***}$$

We have assumed here that the oxygen is not removed by any secondary process and therefore that $P_O = P_{ThO}$.

In the calculations, the approximate equation

$$\log \frac{K_2}{K_1} = \frac{-\Delta H}{2.3\ R} \left(\frac{1}{T_2} - \frac{1}{T_1} \right)$$

(where $K_2 = K_{eq}$ at T_2 and $K_1 = K_{eq}$ at T_1)

was employed using plots of K^{**} and K^{***}. An average value of $\Delta H = 254 \pm 10$ Kcal/mole was obtained for Reaction 6 over the temperature range studied (2513° to 2748° K). The errors shown for values of the heats of reaction for Reactions 1 and 2 have been estimated roughly by choosing several possible lines through the experimental points. An average value of $\Delta H \approx 80$ Kcal/mole over the temperature range 2513 to 2748° K is obtained for Reaction 7 both from the log K^{***} plot and the difference in the heats of Reactions 5 and 6.

The data points obtained for iridium are too scattered to permit determination of the heat of vaporization of iridium from this study. The data are not, however, inconsistent with the heat of vaporization of 155 Kcal/mole obtained in the simple effusion studies.

The estimated ionization cross sections for a number of the elements, by Otvos and Stevenson,[3] may be extrapolated on a plot of cross section, σ,

[3] Otvos, J. W. and D. P. Stevenson, J. Am. Chem. Soc., 78, 546, (1956).

WADD TR 60-463 Pt I

versus atomic number, to obtain, very approximately, the ionization cross section of Th as 150, of O as 3.3, and of Ir as 80. If the usual assumption that atomic ionization cross sections are approximately additive is made, the cross section of ThO and ThO$_2$ may be taken as approximately equal since the oxygen contribution is small.

Also, since by definition

$$P_{ThO_2} = K \frac{I^+_{ThO_2} T}{\sigma_{ThO_2}}$$

and

$$P_{Ir} = K \frac{I^+_{Ir} T}{\sigma_{Ir}} \, ,$$

then

$$P_{ThO_2} = \frac{I^+_{ThO_2} T}{I^+_{Ir} T} \quad \frac{P_{Ir} \, \sigma_{Ir}}{\sigma_{ThO_2}} \, .$$

Substituting numerical values from the appropriate data in these equations, we find the approximate absolute pressure of ThO$_2$ at 2500° K to be 4 x 10^{-4} mm Hg. In a similar manner, the pressure of ThO is found to be approximately 3 x 10^{-4} mm Hg at 2500° K.

It appears from the experimental observations that a reaction occurs between tungsten and thoria at temperatures near 2200° C and higher. From the appearance of the reacted cylindrical crucible, and the fact that there is an induction period before an increase in the rate of vaporization occurs, we may infer that a diffusion controlled process is involved. It is difficult, at present, to say just what is diffusing from the tungsten - thoria interface through the thoria. One possibility is that thorium metal is involved. Thorium metal may then alloy with the iridium within the cell to yield a solution with a lower melting point and equilibrium vapor pressure of iridium than that of pure iridium. The thin, split crucible in Figure 1 (1/16 inch) would be associated with a much smaller induction period if a diffusion mechanism were important.

Since no erosion was observed in the crucible for which we have given

data, we have assumed that the run was completed before the new vaporization mechanism started. The data are, of course, tentative, since the effusion hole was large and there was a definite possibility of interaction with the container material.

5. Al_2O_3

Initially, several mass spectrometric test studies of the vaporization of Al_2O_3 were made in tungsten effusion cells. At temperatures in the vicinity of 2000° C, a major peak at mass 27 (aluminum) was observed with minor peaks at masses 43 (AlO) and 70 (Al_2O). The ratio of the intensity of the Al to the intensity of the AlO or the Al_2O peaks was roughly 1:10. It was observed visually that some reaction had taken place between the Al_2O_3 and the tungsten container. In order to determine whether the species present were due principally to the simple decomposition of the Al_2O_3 or to interaction with tungsten, the vaporization of Al_2O_3 was studied from some simple effusion cells constructed of iridium. These cells were 1/8-inch cylinders of iridium closed at one end. The qualitative results obtained from this study indicated that the ratio of Al to AlO and Al_2O was not affected in a major way by the absence of tungsten metal. There was no visible interaction between Al_2O_3 and iridium, and no iridium oxide species were observed.

In these studies, a fairly large CO peak is always observed. This originates both in the tungsten and in the surrounding furnace materials. Since CO yields a peak at $m/e = 16$ due to cracking of the molecule by the electron beam, and because there is residual oxygen in the instrument, we are not able to observe the effusion of oxygen from the effusion cell. The addition of fast differential pumping to the system did not remedy the situation.

In order to study the interaction of Al_2O_3 and tungsten in somewhat greater detail, effusion cells consisting of the tungsten outer container, shown in Figure 1 and 2 were used. A mixture of Al_2O_3 and tungsten powder was placed inside the effusion cell. In Table 4 we have tabulated the mass spectrometer data obtained from such a study. The data are also plotted in Figure 17. Using the estimated electron cross sections of Otvos and Stevenson[3], as in the thoria study, we then estimate that the ratio Al: AlO: Al_2O: WO_2 is 100: 4: 3: 1.6 approximately. In this case an additional error may be introduced by variation in the sensitivity of the mass spectrometer detector with mass. Such an error is probably not serious when masses of similar weight are studied but may be serious when comparing Al (mass 27) with WO_2 (mass 232).

The chemical compatability experiments discussed in Section V have indicated that the reaction products between tungsten and Al_2O_3 may be influenced by the mean free path of the evaporating molecules. In particular,

WADD TR 60-463 Pt I

TABLE 4 VAPORIZATION FROM A MIXTURE OF Al_2O_3 AND W*

$T°K \pm 10°K$	$\dfrac{10^4}{T}$	Al I_{27}^+	$\log I_{27}^+ T$	AlO I_{43}^+	$\log I_{43}^+ T$	Al_2O I_{70}^+	$\log I_{70}^+ T$	$\Sigma I_{WO_2}^+$	$\log \Sigma I_{WO_2}^+$
2126	4.70	≈ 0.4	2.92	---	---	---	---	---	---
2260	4.42	≈ 1.6	3.55	---	---	≈ 0.1	2.34	0.08	2.25
2273	4.40	≈ 1.5	3.52	≈ 0.08	≈ 2.25	≈ 0.10	2.35	≈ 0.12	2.43
2345	4.26	3.9	3.95	≈ 0.2	2.66	≈ 0.4	2.95	0.16	2.56
2360	4.24	4.1	3.98	---	---	0.36	2.92	0.42	2.99
2389	4.18	5.1	4.07	0.4	2.97	0.63	3.17	0.68	3.20
2441	4.09	7.3	4.24	0.78	3.30	0.88	3.32	0.84	3.30
2495	4.01	9.2	4.35	1.0	3.39	1.4	3.53	1.3	3.50

*1/8-inch orifice in cylindrical cell of 3/16-inch height and inner diameter.
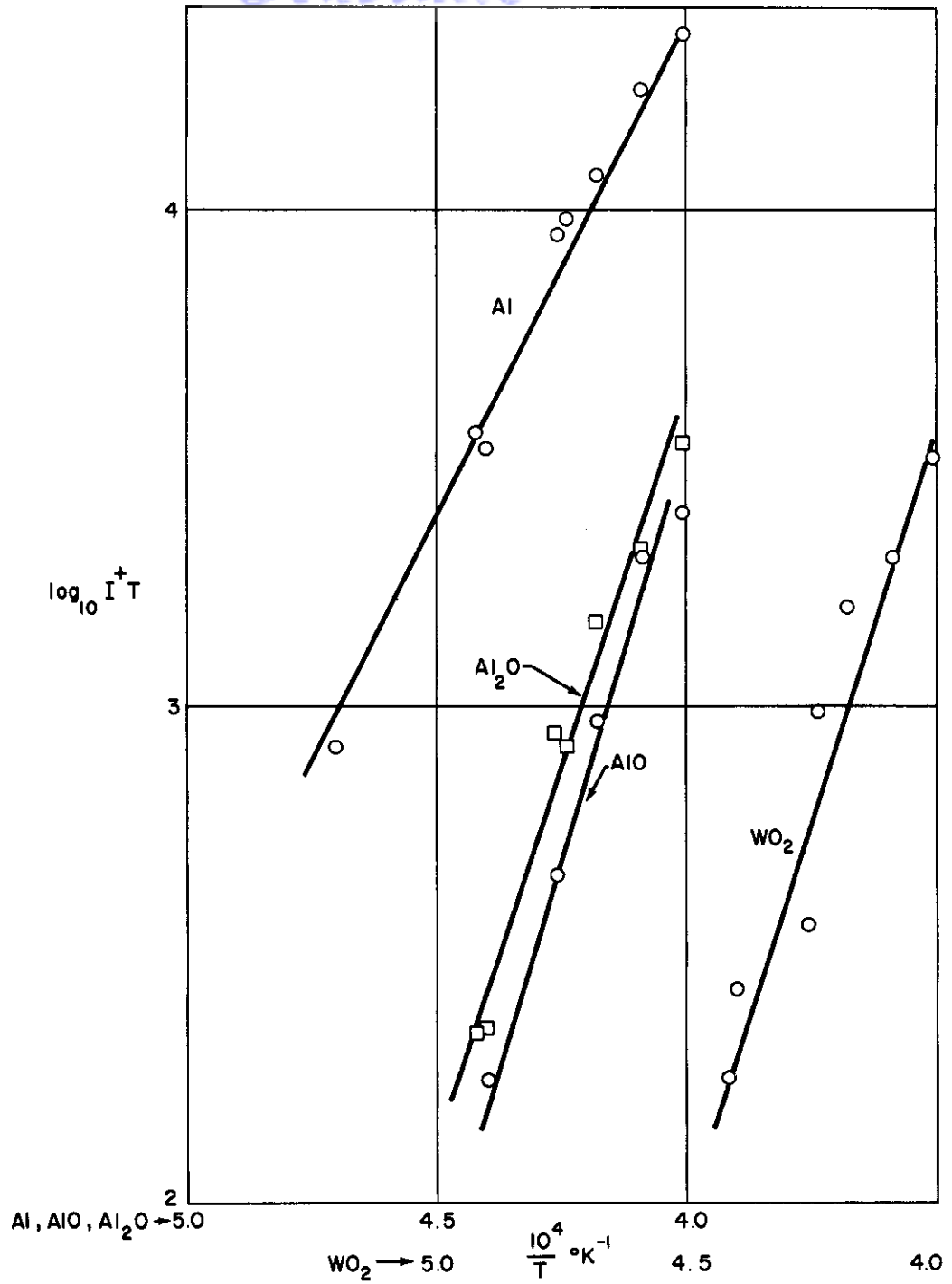
Figure 17 THE VAPORIZATION OF A MIXTURE Al_2O_3 PLUS TUNGSTEN

WADD TR 60-463 PtI

-35-

it appears that the tungsten species may decompose to yield tungsten metal upon contact with a surface.

If this were true, we would find that in an effusion study, which is designed in such a manner that the vapor molecules must strike the wall before effusing out of the system, no tungsten species would be detected. We are therefore not using the above data for thermodynamic calculations until we have determined the role of the tungsten species.

It will be necessary, when we have obtained such information, to also per- form effusion studies to obtain a mass balance in order that the quantity of oxygen effusing from the cell may be determined and that absolute pres- sures may be obtained.

C. FUTURE WORK

Studies of the vaporization of Ir , Os , and other metals in this group should be continued. Iridium outer liners for the thoria effusion cells have been ordered for this purpose. With containers of iridium, it should be possible, by employing radioactive tracers, to study the vaporization of these metals at temperatures as high as 2600° K. The effusion orifice diameter should be varied in some of these experiments. If time permits, studies of the vaporiza- tion of these materials from graphite containers should also be undertaken in order to obtain information about the properties of the carbides.

Studies of the vaporization of ThO_2 both in contact with powdered tungsten and in iridium effusion cells should be undertaken in order to elucidate the vapori- zation of thoria and its interaction with tungsten in greater detail.

Studies of the vaporization of Al_2O_3 both in contact with powdered tungsten and in iridium effusion cells should be undertaken. This should include work with special effusion cells which insure that there is no direct line of sight from the reacting materials to the electron beam.

The surface tension and density of refractories are being determined by the sessile drop method. From the equations of Bashforth and Adams[4] and Dorsey[5], one can obtain the surface tension and density from measurements of the maximum diameter of the drop and height of the apex of the drop above the maximum diameter providing the contact angle is greater than 90 degrees. These dimensions are obtained by photographing the drop while at temperature.

Figure 18 shows a typical photograph of a sessile drop with the dimensions necessary for determining the surface tension from Dorsey's[5] equation:

$$\gamma = g\,d(x)^2 \left(\frac{0.0520}{f}\right) - 0.1227 + 0.0481f$$

where γ is the surface tension in ergs cm^{-2}, g is the acceleration due to gravity, d is the density in $gm\text{-}cm^{-3}$, x is the maximum diameter of the drop, and

$$f = \frac{Z}{x} - 0.4142$$

where Z is the distance from the apex of the drop to the intersection of the 45° tangent with the principal axis.

The furnace, as shown in Figure 19, is comprised of an outer quartz envelope, an inner zirconia heat shield and a tungsten susceptor supported by refractory end pieces. A sight port at one end is utilized to read temperatures optically and for photographing the drop. The furnace is heated inductively, and is capable of temperatures in the 2600 °C range. The drops are photographed with a Praktina FX 35mm camera through a system of optics. The optical system consists of a 463 mm objective lens and the 58mm camera lens. The camera and objective lens are rigidly mounted on an optical bench so as to obtain a 4X magnification. A drop size of 0.5cm will approximately fill the frame of 35mm film. A high contrast extreme resolution film is used, and the dimensions are read from the developed film with a Jarrell-Ash microphotometer.

Two attempts have been made to measure the surface tension of fused silica.

In the first run, a wetting drop for which the Dorsey[5] equation does not hold was formed on a tungsten foil substrate.

---

[4]Bashforth and Adams, An Attempt to Test the Theories of Capillary Action, Cambridge, (1883).
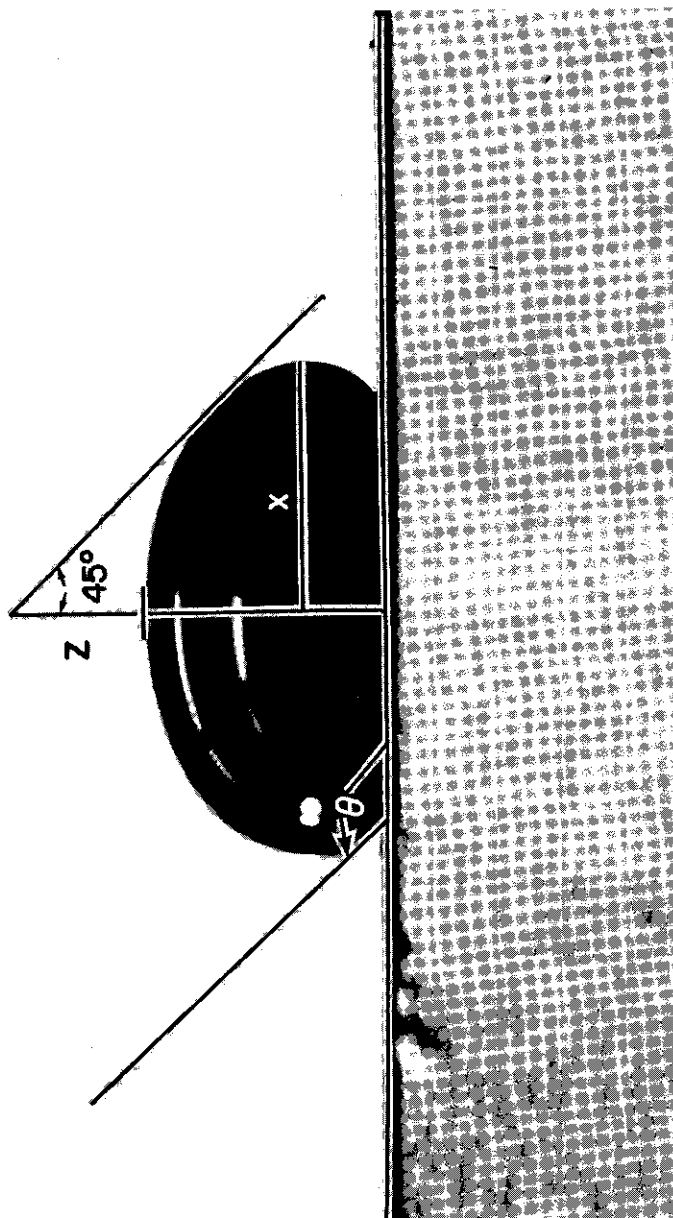
[5]Dorsey, N.E., J. Wash. Acad. Sci., 18, 505-9, (1928).

WADD TR 60-463 Pt I

Figure 18 SESSILE DROP
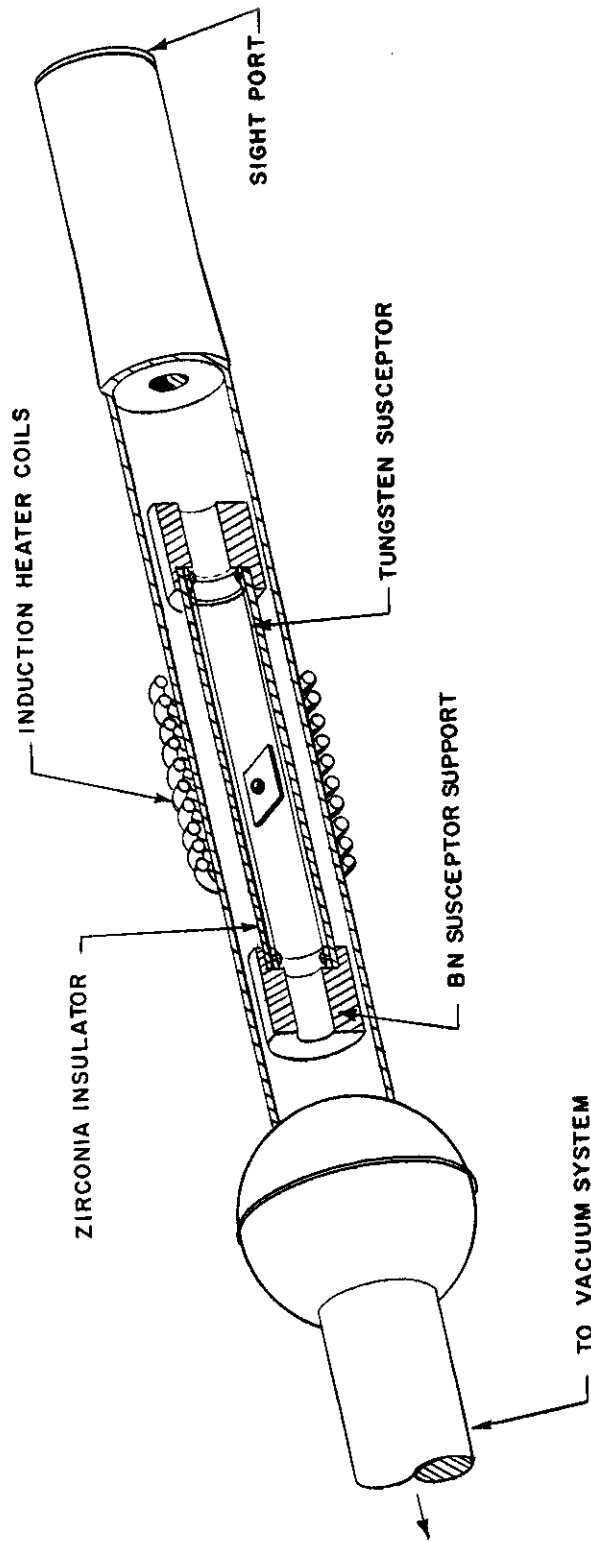
-38-

SIGHT PORT

TUNGSTEN SUSCEPTOR

INDUCTION HEATER COILS

BN SUSCEPTOR SUPPORT

ZIRCONIA INSULATOR

TO VACUUM SYSTEM

Figure 19 SESSILE DROP EQUIPMENT

WADD TR 60-463 PtI

-39-

In the second run, the tungsten elements were in direct contact with the zirconia. A reaction occurred at elevated temperatures, between the zirconia and tungsten, making it impossible to carry out the experiment. Samples of the reacted area were analyzed and the results reported under compatability studies. Due to this reaction, opaque quartz tubing will be used as a heat shield in place of the zirconia.

WADD TR 60-463 Pt I

The viscosity of fused silica has been measured in the temperature range of 1935 to 2560°C. The results were determined by a counterbalanced sphere method similar to that employed by Shartsis and Spinner.[6] This method consists basically of determining the viscosity of the fluid by measuring the force necessary to move a counterbalanced sphere up or down in the molten fluid with a constant velocity. The system was calibrated at various temperatures with known viscosity National Bureau of Standards oils.

Figure 20 shows the apparatus employed. It consists of a standard analytical balance, an aircooled quartz furnace system, a source of purified argon, and an induction heating unit. The pan was removed from one side of the balance and replaced with a tungsten rod and sphere. A tungsten crucible mounted on a zirconia pedestal placed inside an opaque quartz heat shield was mounted, as shown in the quartz furnace tube. Facilities attached at the top of the furnace allow for the evacuation of the system, for outgassing, and the introduction of purified argon used in the actual run. Temperatures are read through a sight port on the bottom of the furnace with a "Pyro" micro-optical pyrometer. The furnace was heated inductively with the tungsten crucible as the suscepter, and cooled by two floor fans.

Before each run, the tungsten crucible was outgassed at 2600°C at pressures of 10^{-4} mm of mercury. After cooling the crucible, the quartz sample was added and outgassed at 1500°C at approximately the same pressures as the crucible. After the outgassing procedure, purified argon was introduced. The gas was purified by passing it through an electrodryer containing activated alumina, to remove water, then through two sealed stainless steel tubes, containing calcium chips, and heated to 600 and 350°C respectively, to remove nitrogen, oxygen, and hydrogen. At this point, the ball and rod were introduced and the furnace temperature raised. When the temperature was above the softening point of silica, the ball was lowered into the center point of the fluid by adjusting the lab jacks. After allowing the system to reach an equilibrium temperature, the ball was set in motion by adding or removing weights from the right hand pan. The ball's velocity was obtained by timing the balance pointer motion through ten scale divisions. Weight versus velocity was plotted from the data obtained for a rising and descending sphere. Figure 21 shows a typical plot at temperature. The process was repeated at each temperature and slopes thus determined. Brightness and emissivity corrections were made for all observed temperatures.

The results for fused silica and other glasses determined on this contract and in previous work are shown in Table 5 and Figure 22 compared to results of previous investigators.

---

[6]Shartsis, L. and Spinner S., Viscosity and Density of Molten Optical Glasses, J. Research NBS 46, 176 (1951).
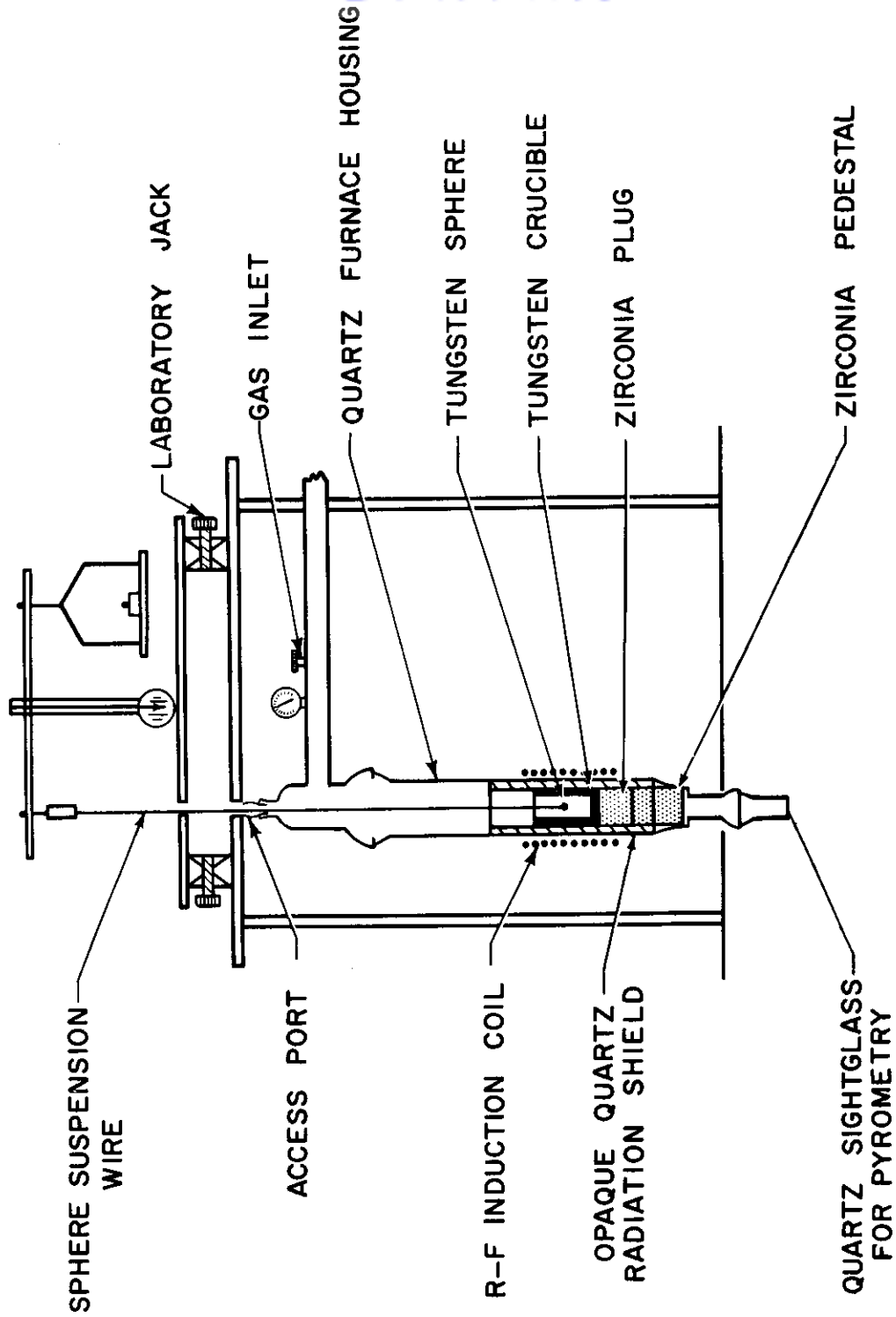
WADD TR 60-463 Pt I
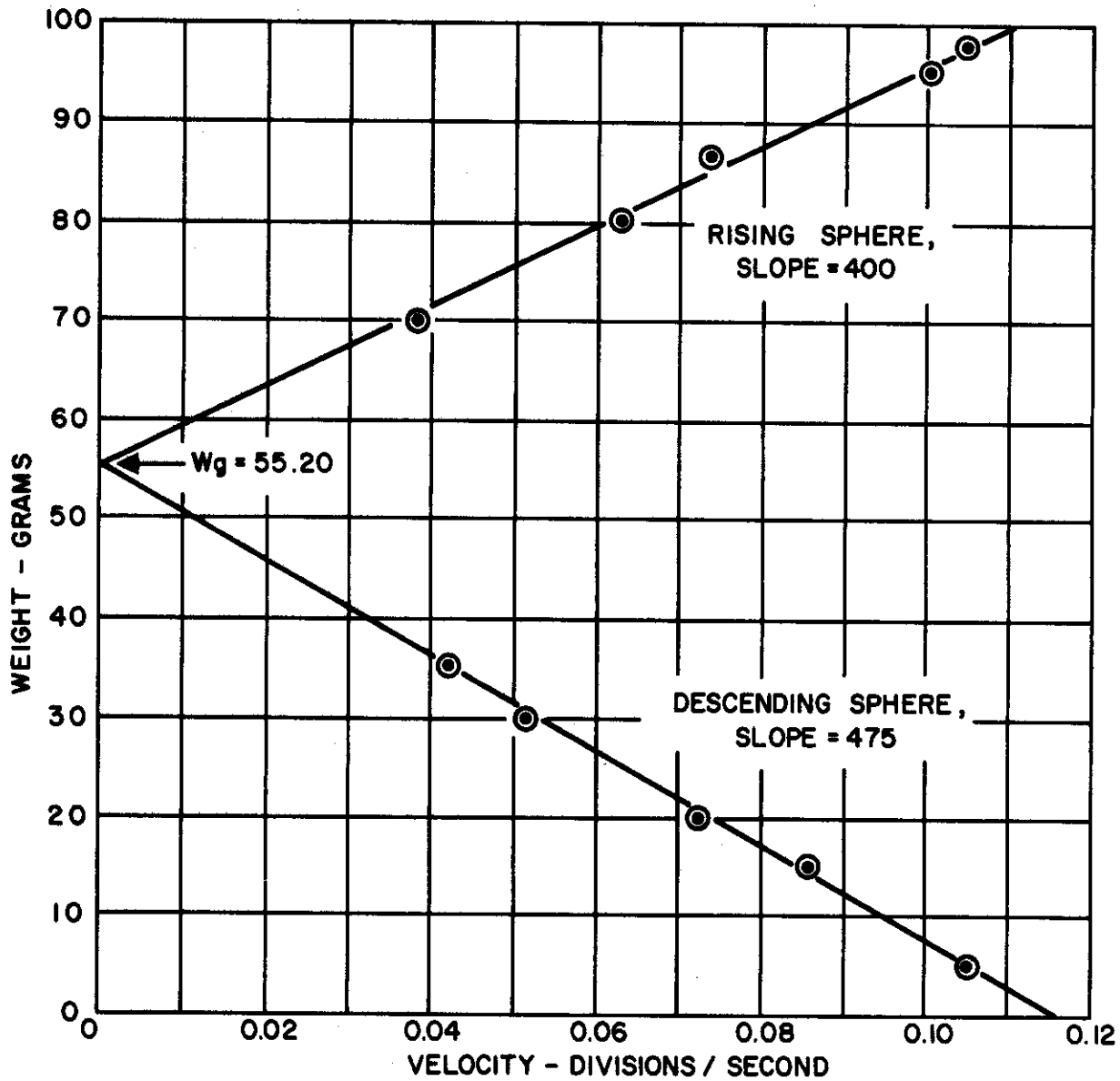
Figure 20 COUNTER-BALANCED SPHERE APPARATUS FOR DETERMINING VISCOSITY

LABORATORY JACK

GAS INLET

QUARTZ FURNACE HOUSING

TUNGSTEN SPHERE

TUNGSTEN CRUCIBLE

ZIRCONIA PLUG

ZIRCONIA PEDESTAL

SPHERE SUSPENSION WIRE

ACCESS PORT

R-F INDUCTION COIL

OPAQUE QUARTZ RADIATION SHIELD

QUARTZ SIGHTGLASS FOR PYROMETRY

Figure 21 EFFECT OF WEIGHT ON VELOCITY OF A COUNTERBALANCED
TUNGSTEN SPHERE IN MOLTEN FUSED SILICA AT 2140°C

Figure 22 COMPARATIVE VISCOSITY DATA
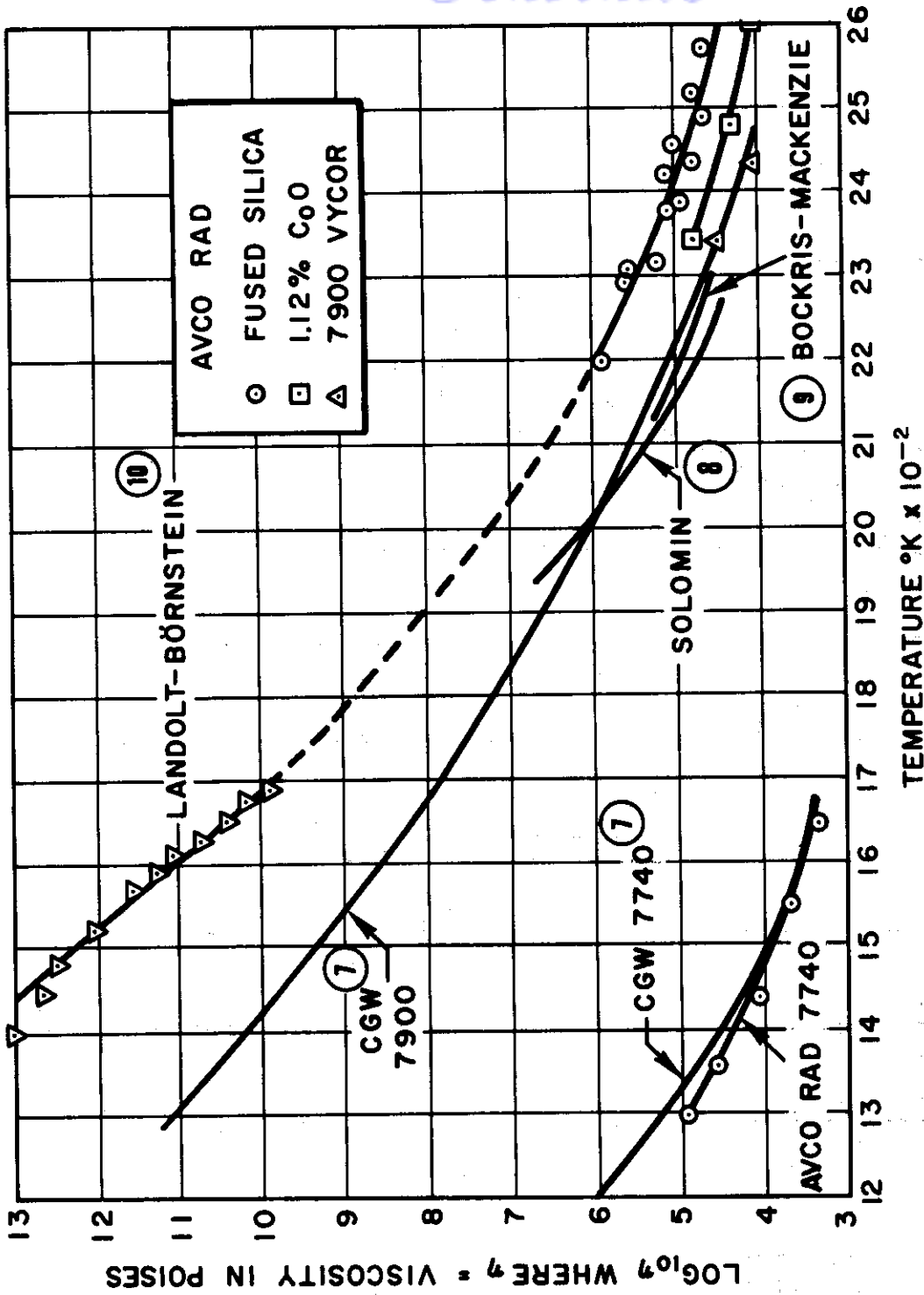
7. Properties of Selected Commercial Glasses, B-83, Corning Glass Works, Corning, N. Y. 1957

8. N. U. Solomin, J. Phys- Chem- (USSR) 14,235 (1940)

9. J. O. M. Bockris, J. D. Mackenzie and J. A. Kitchener, Faraday Soc. 51, 1734 (1955)

10. Landholt-Bornstein, Zahlewerte und Funktionen, Springer Verlag, Berlin (1955), Sechste Auflage, IV Bund, Technik, Teil I, Stoffwerte und Mechanisches Verhalten Von Nichtmetallen Fig. 42242, Pg 632

WADD TR 60-463 PtI

-44-

TABLE 5 EXPERIMENTAL RESULTS AT THIS LABORATORY FOR THE VISCOSITY OF FUSED SILICA AND OTHER GLASSES AS A FUNCTION OF TEMPERATURE

	$Log_{10}\eta$ (Poises)	$T°K$
<u>Fused Silica</u>	5.858	2208
	5.552	2321
	5.450	2328
	5.120	2333
	5.036	2387
	4.867	2398
	5.070	2428
	4.784	2443
	4.992	2460
	4.635	2501
	4.699	2530
	4.632	2595
<u>SiO_2 + 1.12% CoO</u>	4.720	2363
	4.305	2503
	4.086	2623
<u>CGW Vycor 7900</u>	4.585	2364
	3.995	2459
<u>CGW Pyrex 7740</u> [7]	5.060	1319
	4.636	1373
	4.131	1460
	4.188	1463
	3.656	1566
	3.341	1662

The counterbalanced sphere apparatus is used for measuring the viscosity of very viscous materials. For more fluid materials, we are using an oscillating bob viscometer. The apparatus is shown in Figures 23 and 24. A bob, that is rigidly attached to the magnet and mirror and suspended by a torsion wire, is made to oscillate in the molten material. The bob is set into oscillation by moving the micrometer head so that the magnet and solenoids are coaxial. Enough current is then fed into the solenoids to keep the system rigid while tension is put into the wire by means of the micrometer. After all vibrations have been damped out, the solenoid current is stopped and the system starts oscillating. This procedure allows one to transmit almost pure oscillation to

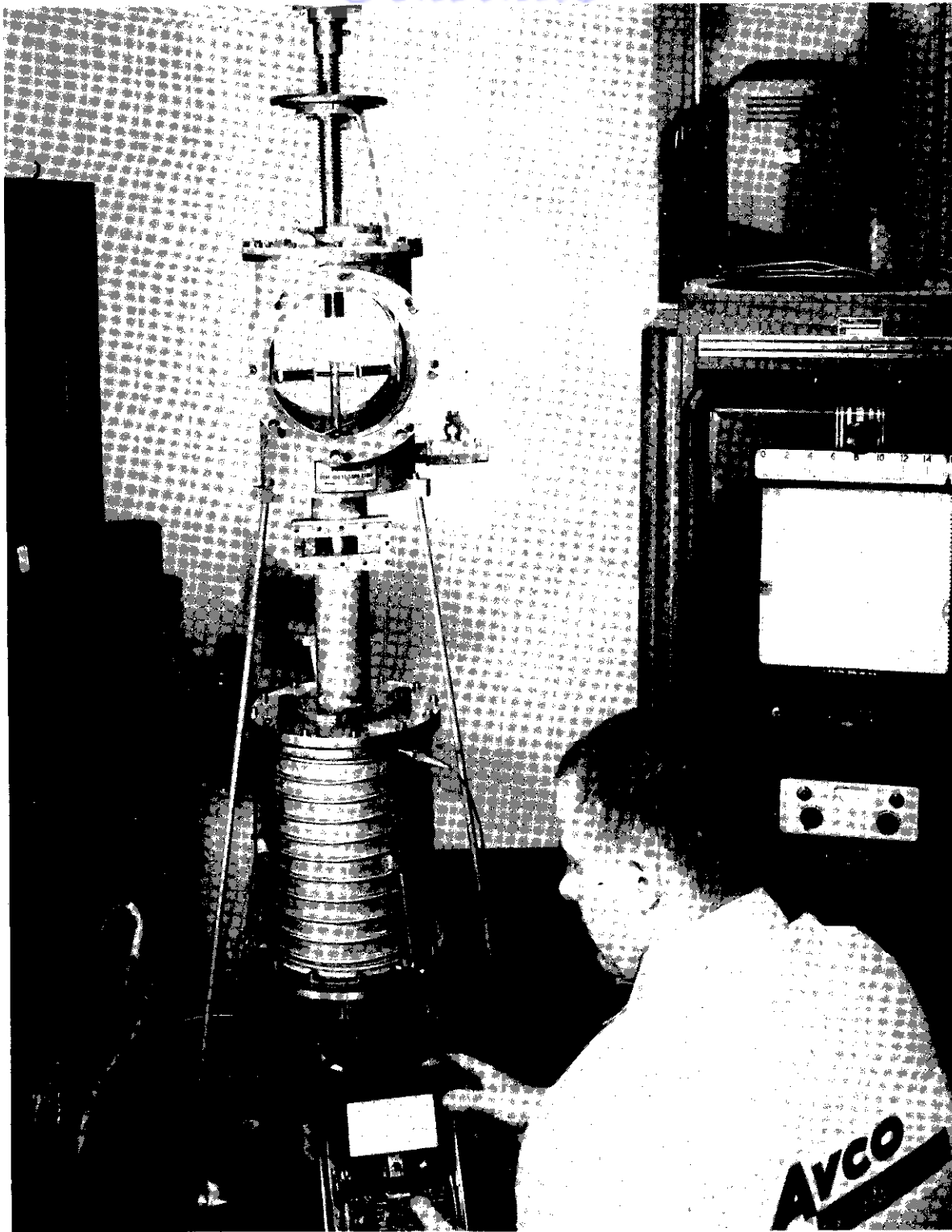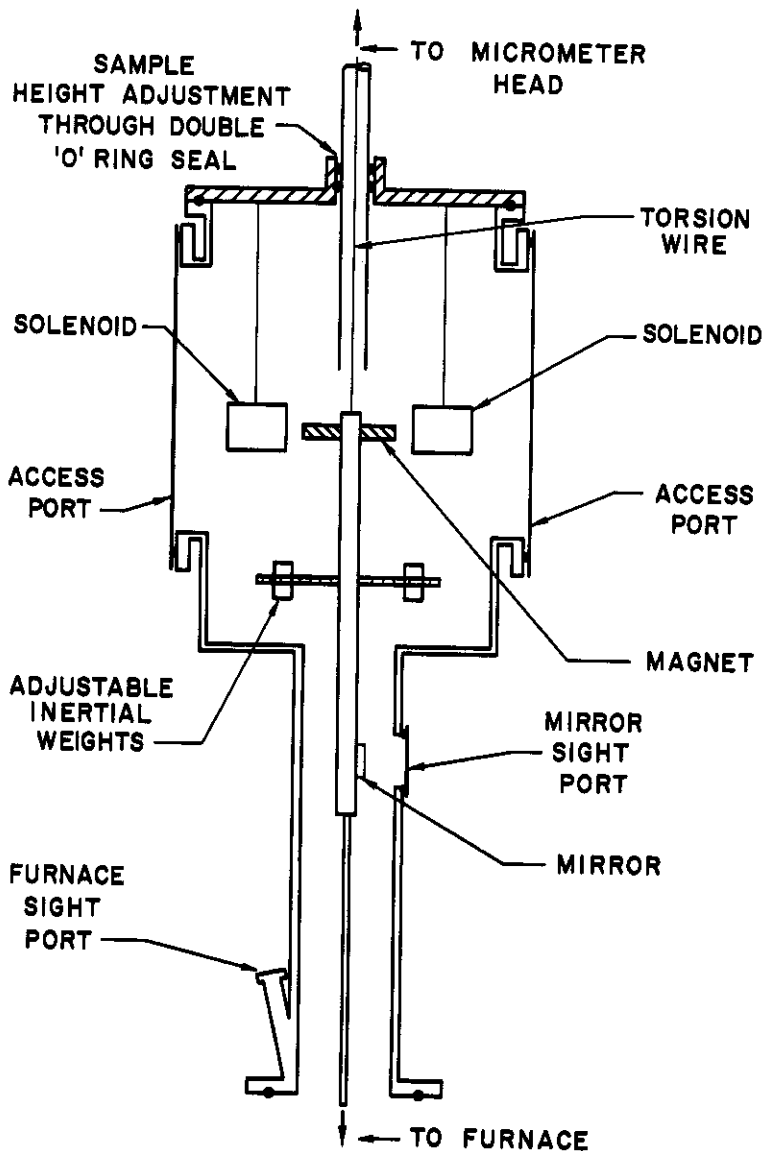[7] Properties of Selected Commercial Glasses, B-83, Corning Glass Works, Corning, N. Y., (1957).

WADD TR 60-463 Pt I

Figure 23 VISCOMETER

Figure 24 VISCOMETER

the system with very little pendulum like motion. The periods and amplitudes of the oscillations are monitored through the sight port.

Oils of known viscosity have been used to determine the constants of the equation

$$\eta = \frac{(IK)^{1/2}}{C} \lambda$$

where

η = viscosity (Poises),

I = moment of inertia (gm -cm^2),

K = torsional constant of wire (dyne - cm/unit twist),

C = apparatus constant (cm^3),

λ = logarithmic decrement of the amplitude.

The viscosity of molten alumina was determined with this apparatus as 13 poises at temperatures of 2075 to 2200° C. The material solidifies rapidly over a very small temperature range. This value is probably reliable to ±100 percent at the present time. The alumina was contained in an iridium crucible and a 1/16-inch iridium rod was used as a bob. The alumina was cream colored after the experiment and contained a number of voids. Attempts will be made to refine the data by trying to eliminate the voids.

WADD TR 60-463 Pt I

-48-

The counterbalanced sphere apparatus has been successfully utilized in measure-
ing electrical conductivities. The measurements are made with an Industrial
Instrument RC16B conductivity bridge. The unit has a built-in oscillator and
null indicating device which facilitates the determinations. Results have been
obtained on Corning Glass Works 7900 Vycor and 7740 Pyrex. The relationship
between $\log_{10}$ volume resistivity and the reciprocal of the absolute temperature
is shown in Figure 25. Analysis of these data show that the Rasch-Hinrichsen
Law, ρ = Aexp E/RT, is obeyed. Solving the equation for the activation energy
of resistivity, E, yields 13.8 and 12.2 K Cal/mole for Vycor and Pyrex respec-
tively. The data show that the activation energy decreases with an increase
of metallic oxide additives and the resistivity increases with the higher per-
centage silica content. Spectrographic analysis of the glasses before and after
each run shows no change in the major constituents indicating that no reaction
has occurred during the course of the run.

Calibration of the cell constant has been performed with normal solutions of
KCl at room temperatures, and the factors applied in the calculations. Cor-
rections were also made for changes in lead resistance at elevated tempera-
tures.

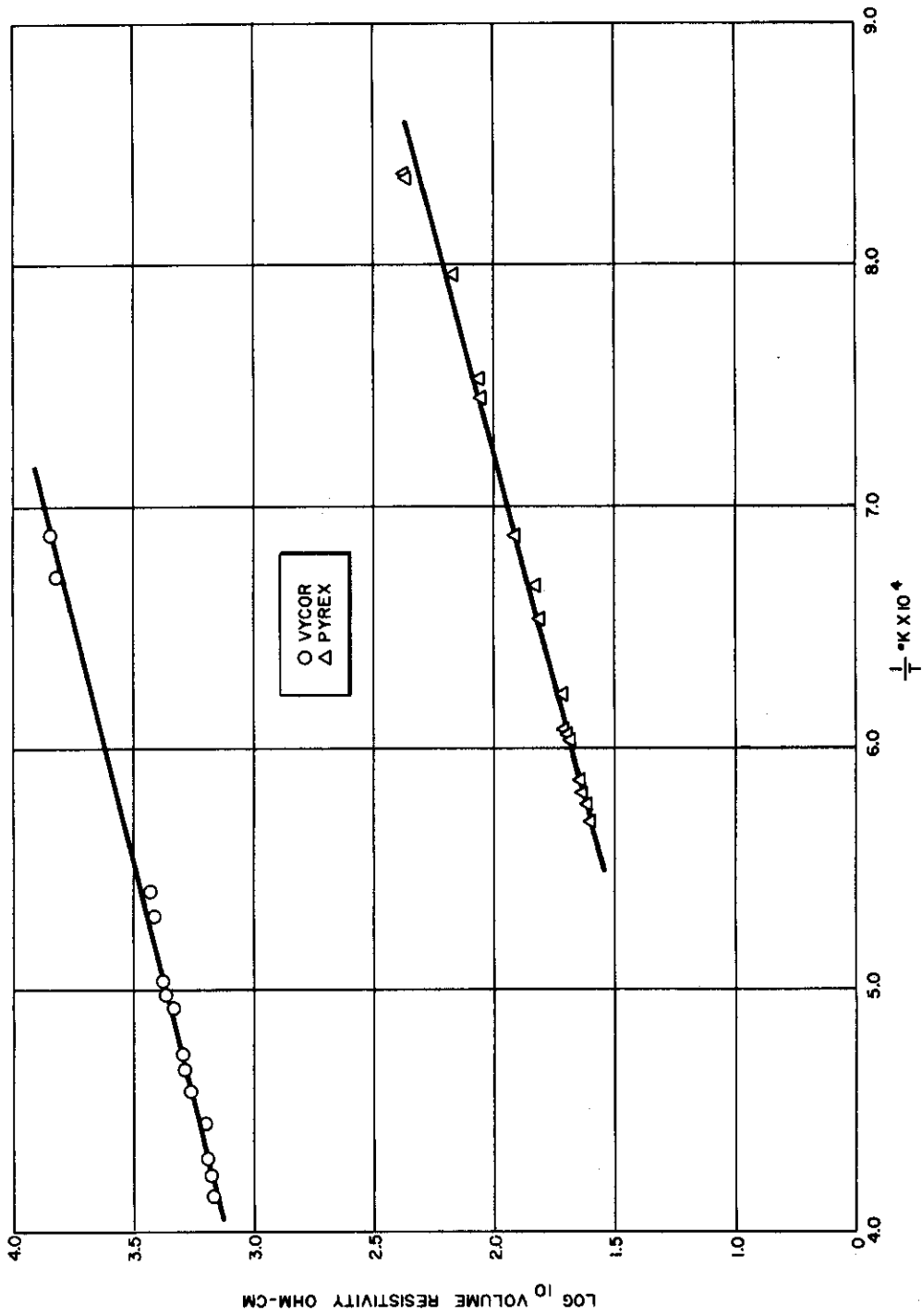Further **studies** will be made on refractories and glasses with added metal
oxides.

WADD TR 60-463 Pt I

Figure 25 1/T VERSUS $\log_{10}$ VOLUME RESISTIVITY, OHM-CM

V. CHEMICAL COMPATABILITY STUDIES

The results of the investigation of the interaction between tungsten and molten alumina can be summarized as follows:

1. Molten alumina reacts with tungsten at the tungsten grain boundaries (intergranular attack).

2. The tungsten is carried through the melt by means of an intermediate with a high decomposition pressure.

The experiments in question involve melting charges of recrystallized alumina rods* in a tungsten crucible**. The tungsten crucible is suspended in a quartz envelope and heated inductively.

Figure 26 shows photomicrographs of the tungsten-alumina interface and are typical of systems showing intergranular attack.

In all experiments in an argon atmosphere where the entire charge is melted, the tungsten covers the entire upper surface with a continuous film, as shown in Figure 27a. In experiments where alumina is fused in vacuum in a tungsten crucible, the tungsten film is not observed at the upper surface. However, as shown schematically in Figure 28a, and in a photograph in Figure 28b, a similar film is observed on the upper surface of any large voids that occur in the melt. The film grown in vacuum has many nodules attached to it as shown in Figure 28b.

A plausible interpretation of these results is that the tungsten is dissolved by the intergranular attack of molten alumina on it, and that it goes into solution in some form other than tungsten. This tungsten bearing species is postulated to be in equilibrium with a vapor that readily disproportionates into tungsten metal (and some other constituent).

This reaction mechanism explains all the experimental results.

In vacuum where the mean free path is large, the tungsten bearing species and/ or its decomposition products are carried away so that a tungsten film does not form at the surface.

In an inert atmosphere, in a covered crucible in vacuum, or inside a void where the mean free path is small, the tungsten is reflected back to the surface where it precipitates in the form of hexagonal growth lamellae, shown in Figure 29.
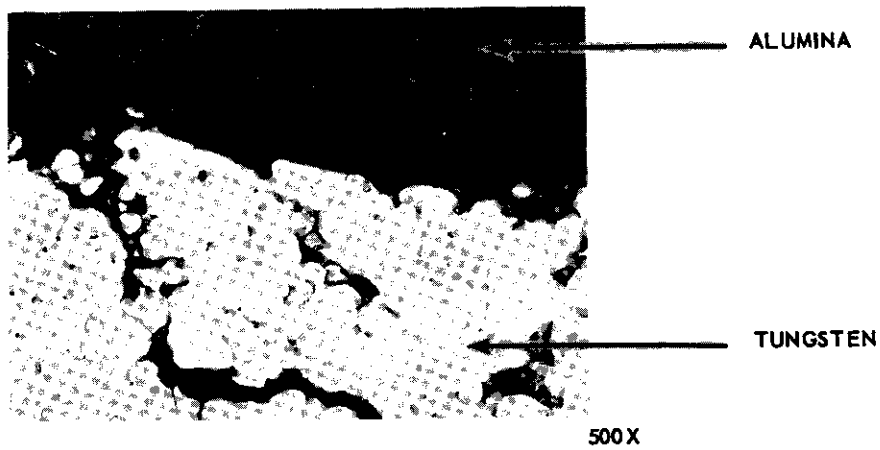
---

*Recrystallized Al_2O_3 -R.R. Morgan Co.

**Arc Cast Tungsten-General Electric Co.
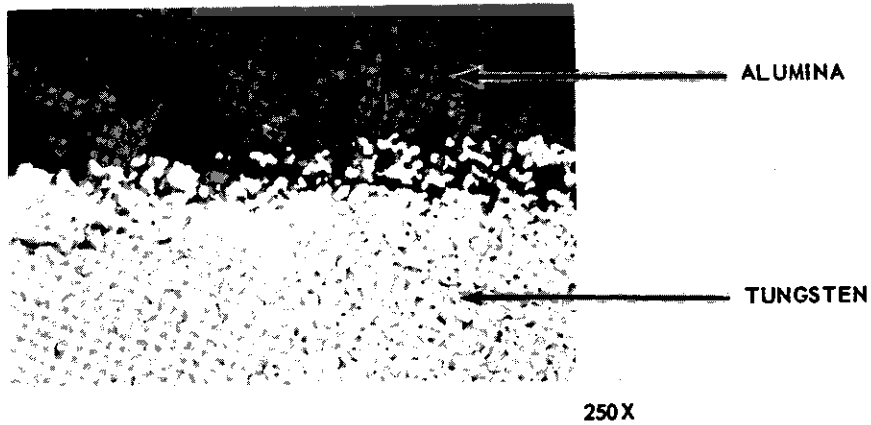
WADD TR 60-463 Pt I

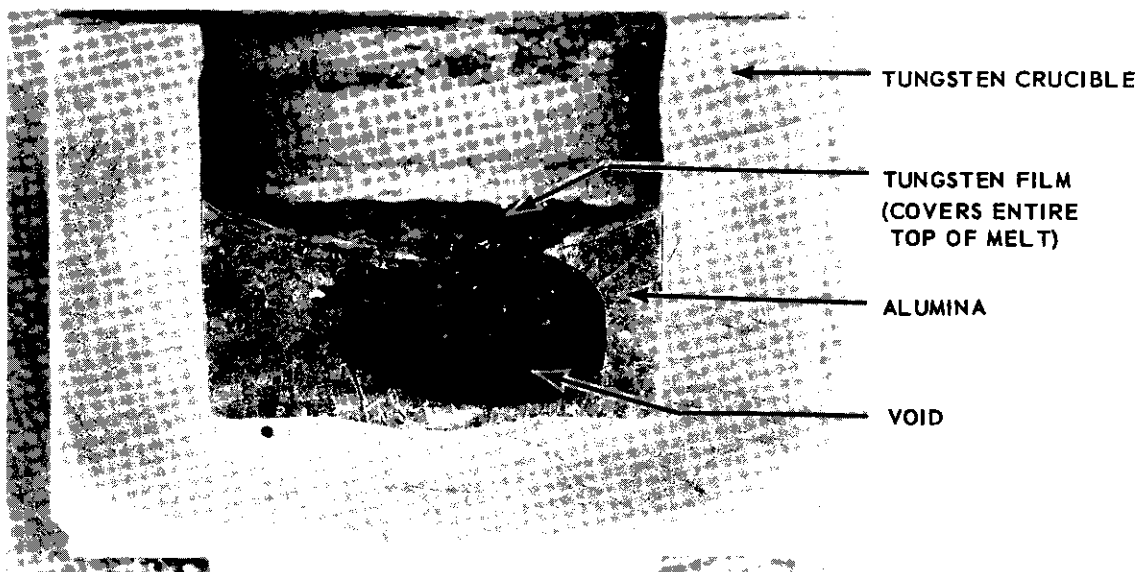-51-

250 X

a. TUNGSTEN-ALUMINA INTERFACE

250 X

b. TUNGSTEN-ALUMINA INTERFACE

500 X
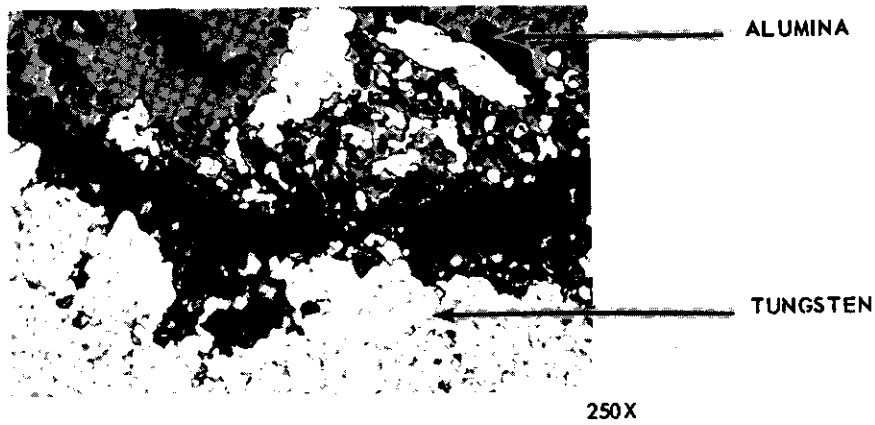
c. TUNGSTEN-ALUMINA INTERFACE

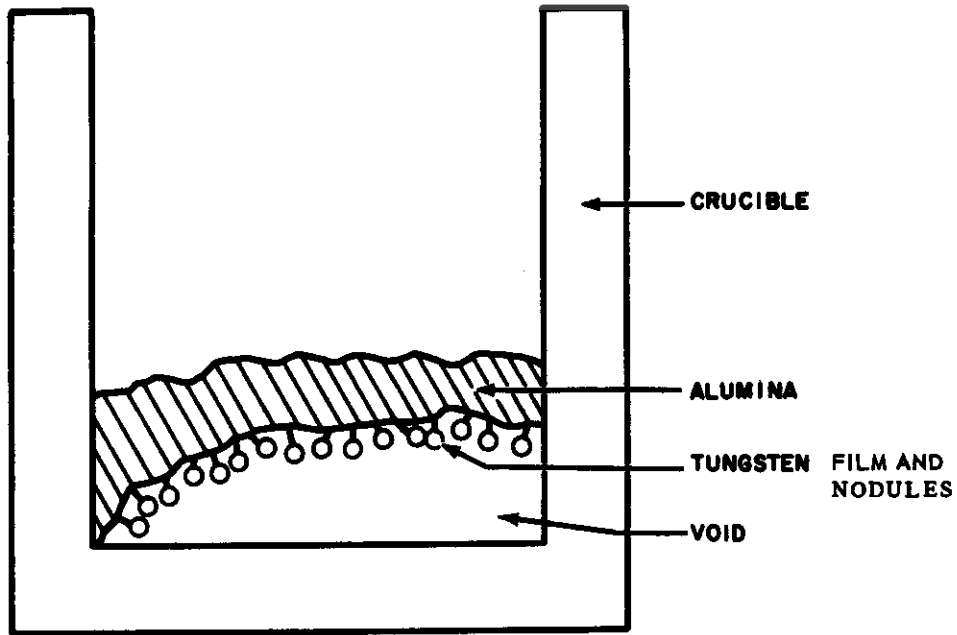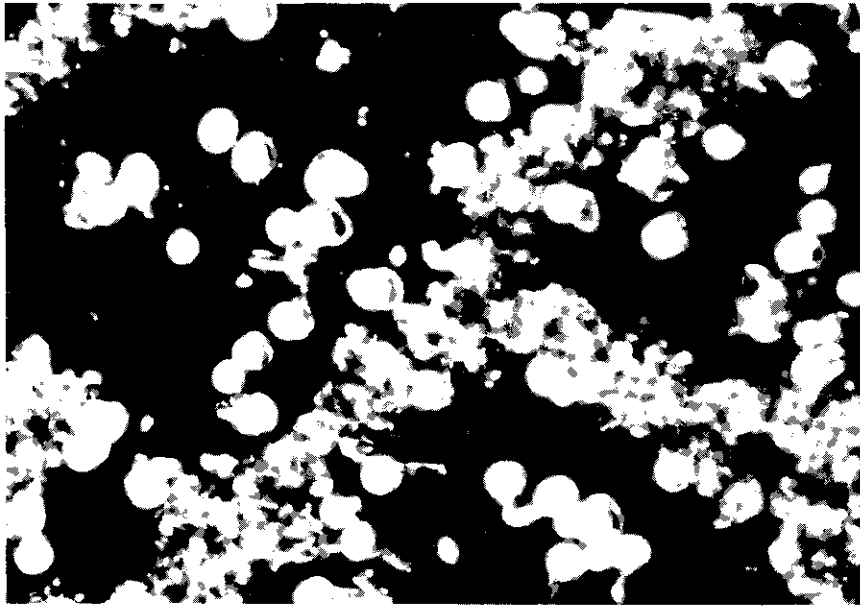Figure 26   INTERGRANULAR ATTACK OF ALUMINA ON TUNGSTEN

WADD TR 60-463 PtI

-52-

TUNGSTEN CRUCIBLE

TUNGSTEN FILM
(COVERS ENTIRE
TOP OF MELT)

ALUMINA

VOID

4X

a.

TUNGSTEN FILM

ALUMINA
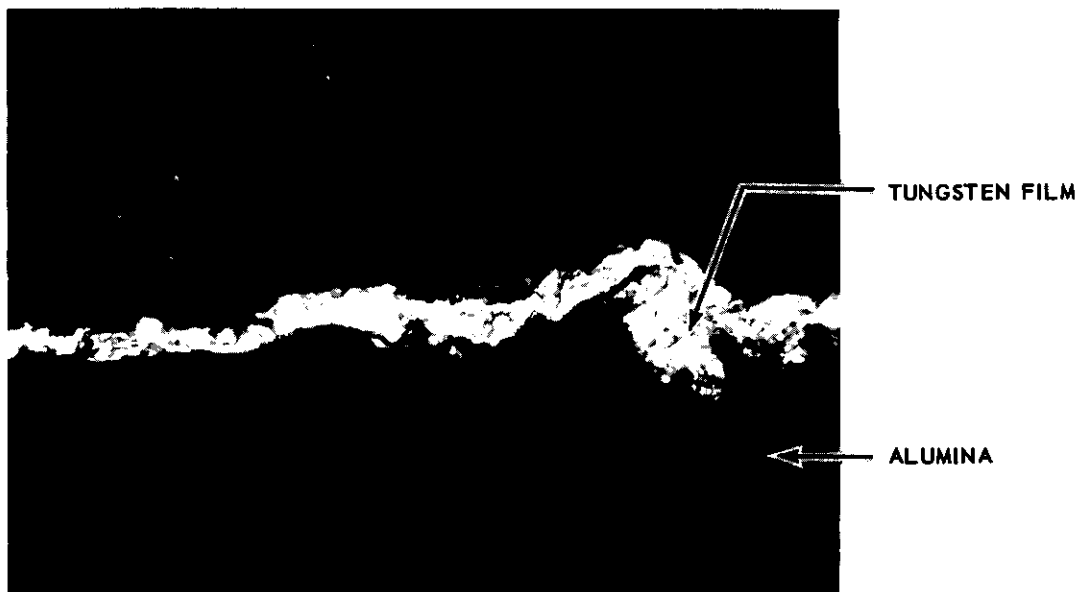
1000X

b.

Figure 27 PHOTOGRAPHS OF TUNGSTEN FILM FORMATION FROM ARGON EXPERIMENT
WADDTR 60-463 PtI

-53-

CRUCIBLE

ALUMINA

TUNGSTEN FILM AND NODULES

VOID

a. SCHEMATIC OF TUNGSTEN FILM

96X

b. PHOTOGRAPH UNDERSIDE OF TUNGSTEN FILM (NODULES)

Figure 28   TUNGSTEN FILM FROM VACUUM EXPERIMENT

WADD TR 60-463 PtI

-54-

100X

Figure 29   TUNGSTEN GROWTH LAMELLAE

WADD TR 60-463 PtI

-55-

This reaction mechanism points out a possible major source of error in the interpretation of Knudsen effusion and Langmuir evaporation experiments. In an open tungsten crucible one may be measuring a higher rate of evaporation of the tungsten complex, whereas, in a closed crucible, where the molecules encounter collisions before leaving the crucible, the pressure may more nearly reflect the decomposition pressure of pure alumina. The placement and size of a Knudsen effusion orifice may lead to cases where one determines a pressure intermediate between the two extreme cases.

Metallographic, spectroscopic, and chemical analysis of samples fused in vacuum and inert atmospheres, have not indicated any attack of molten alumina on iridium. The alumina has an opaque white color after being fused in iridium.

Considerable amounts of boron are dissolved in alumina when it is fused in a boron nitride crucible.

During a surface tension experiment a rather violent reaction occurred in which a molten material formed and was thrown out of the hot zone. This condition was brought about by the experimental setup. The tungsten susceptor which was used was a 5 mil tungsten sheet rolled into a cylinder and placed inside a zirconia tube. Electrical continuity around the perimeter was obtained by a 1/4-inch overlap in the tungsten sheet. When this was heated inductively, it was observed that hot spots formed along the overlap due to the high contact resistance at these points. One of these points was at the front edge of the zirconia pedestal which was used to hold the tungsten substrate for the sessile drop. When the temperature of the tungsten substrate was at about 1800° C the reaction started and small droplets of unknown molten material were hurled out of the hot zone. The temperature of the hot spot was not measured but could have been in the range of 2200 to 2500° C.

Another contributing factor was that the zirconia itself became highly conducting at these temperatures and would have become directly heated by the induction coil.

When the system had cooled, it was disassembled and examined. Melting had obviously occurred inasmuch as the tungsten at some points was completely imbedded in the material. Also, a large round void had formed in the zirconia pedestal.

As yet no definite conclusion can be made as to what actually occurred. It can not be said as to whether there was a reaction between the tungsten and zirconia or whether the zirconia simply melted. At present spectroscopic analysis of the molten material are being made and it is hoped a definite answer to this can be found.

WADD TR 60-463 Pt I

APPENDIX I

NULL POINT TORSION EFFUSION APPARATUS

by   C. Rosen

ABSTRACT

A null point apparatus, capable of manual or automatic operation, for deter-
mining vapor pressures by the torsion effusion method is described.

INTRODUCTION

The most common method for determining vapor pressures of refractory ma-
terials at elevated temperatures is the effusion technique.[1] With this method,
a condensed phase is enclosed in a crucible and the vapors are allowed to effuse
through a small orifice of known dimensions. The force of the issuing beam
depends only upon the vapor pressure in the cell and the dimensions of the ori-
fice[2]. In the conventional torsional effusion method,[3] the force of the beam is
determined by allowing it to flow through two eccentrically located holes in a
crucible suspended from a wire calibrated in terms of force per angular dis-
placement and measuring this displacement. This technique offers an ex-
tremely rapid and relatively accurate method of determining vapor pressures
using very small quantities of material.

The major drawbacks to the method are:

   1.   The torsional constant of the wire is subject to change and also to
   hysteresis effects.

   2.   Only a small fraction of the possible rotation of the suspension is
   visible in most high temperature torsional equipment, and

   3.   Separate torsion wires must be used for different pressures in order
   to stay within the given angular displacement and within a given accuracy.

The null point method described in this article eliminates these objections,
and in addition, is capable of automatically recording the pressure as a
function of time or of temperature.

---

[1]Knudsen, M., (a) Ann. Phys. 28, 75 (1909); (b) Ibid 28, 999 (1909).

[2]Searcy, A.W. and R.D. Freeman, J. Chemical Phys. 23, 88 (1955).

[3]Volmer, M., Physik, Chem. Bodenstein Festband, 836 (1931).
WADD TR 60-463 Pt I

APPARATUS

The apparatus is shown schematically in Figure 1.

The torsion suspension wire is connected at one end to a micrometer head and at the other end to an aluminum rod to which is rigidly attached an Alnico V magnet. When measurements are being performed, the axis of this magnet is kept coaxial with that of the two surrounding solenoids. The effusion cell is rigidly mounted to the aluminum rod to which a mirror is cemented that can be viewed through a sight port that allows one to view 120 degrees of rotation.

MANUAL OPERATION

Place the sample in the cell and evacuate the system. Rotate the micrometer head until the solenoids and magnet are coaxial. Adjust the furnace temperature and pass enough current through the solenoids to exactly counterbalance any torsional force due to effusion. Any movement of the cell is determined by viewing the cross-hair on the mirror.

The solenoids are wound in series to keep their magnetic fields equal in order to avoid introducing torques into the system. It has been shown that, for a fixed geometry, the force between the magnet and the solenoids is proportional only to the current going through the solenoids.[4] Therefore, for a given system, the vapor pressure is directly proportional only to the current going through the solenoids. This current is determined by measuring the voltage drop across a standard resistance in series with the solenoids.

The constants of the system are determined by calibration with materials of known vapor pressure.

AUTOMATIC OPERATION

If the deflection of the effusion cell is detected photoelectrically, the arrangement shown in Figure 2 can be used to keep the system continuously in balance.

As the suspension shifts, due to an increase in the torsional force, there is an increase in the light to one of the photoelectric cells which increases the current through it. This increased current causes a thyratron to become conductive and energize a relay which starts a motor turning. The motor turns a potentiometer that varies the current in the solenoids in such a way as to reverse the direction of rotation of the suspension.

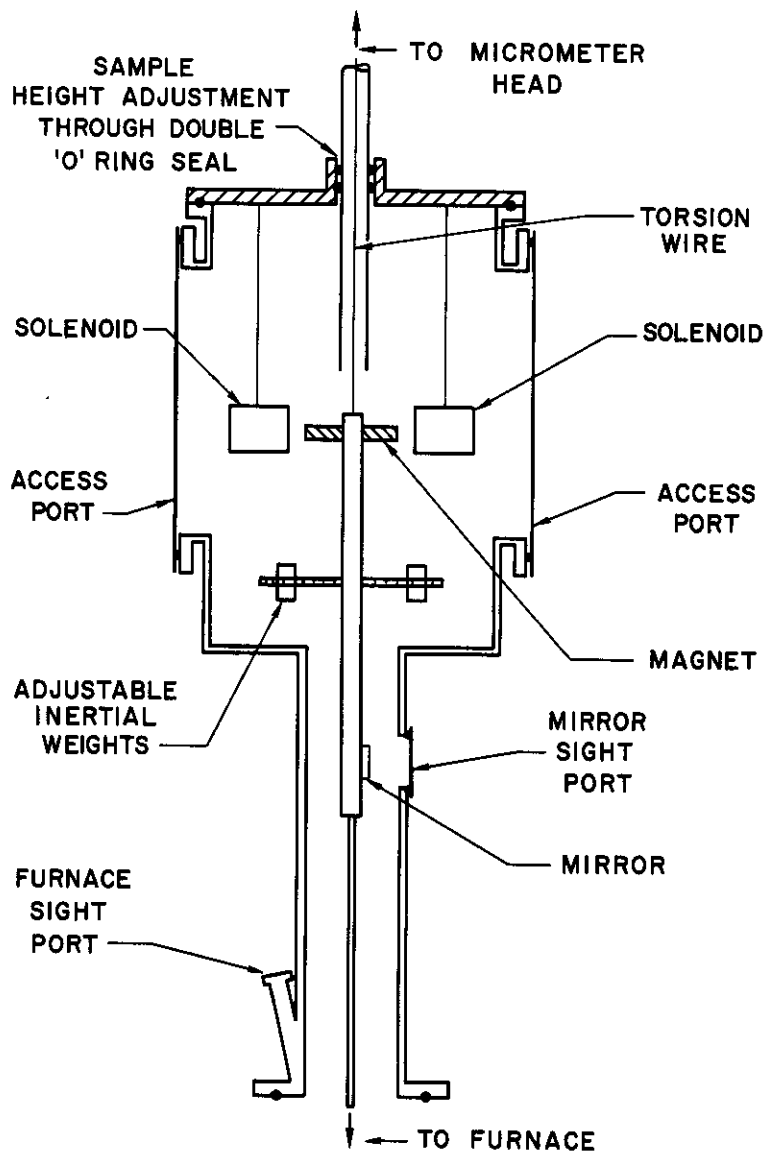[4]Mauer, F. A., Rev. Sci. Inst., 25, 598 (1954).

WADD TR 60-463 Pt I

Figure 1 NULL-POINT TORSION EFFUSION APPARATUS

-59-
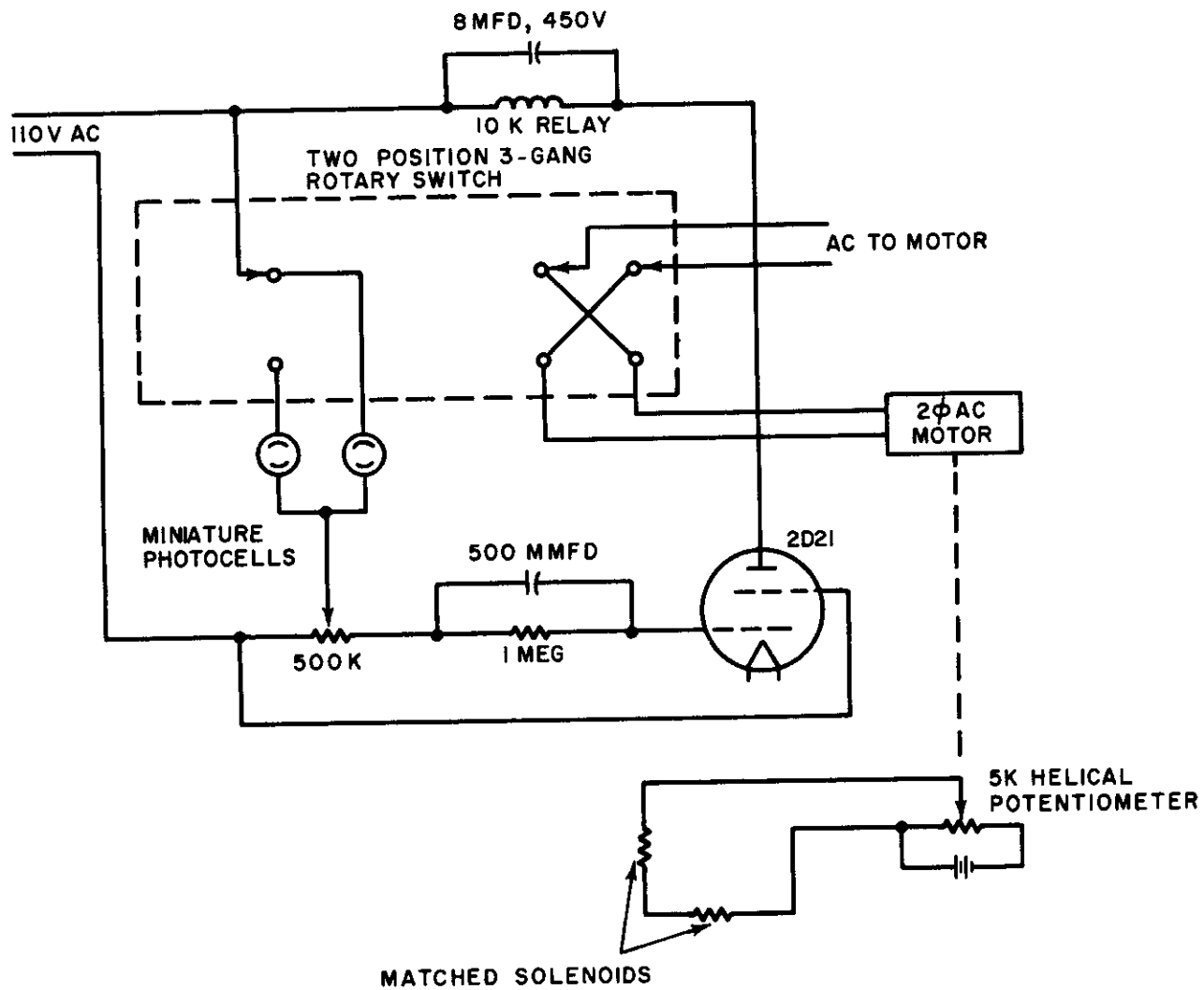
Figure 2 CONTROL CIRCUIT

When the system rotates past the null position in the opposite direction, the light to the other photocell increases, and the thyratron again becomes conductive, the relay to the motor is energized and the motor reverses direction.

The current going through the solenoid is monitored on a strip chart recorder to give a continuous record of pressure versus time. If, in addition, the temperature is continuously monitored, the pressure versus the temperature can be plotted on the recorder.

DISCUSSION

The major drawbacks to the torsional method, listed in the introduction, are eliminated by counterbalancing with electromagnetic force the torsional force due to effusion.

The wire now acts as a bearing, and its torsional constant influences only the lower limit of the sensitivity of the system. The more flexible the wire, the greater is the sensitivity.

Thus a single suspension wire can be used for all experiments since the force between the magnet and solenoid is determined only by the current going through the solenoid.

The magnet and solenoids also act as a damping device to eliminate many of the extraneous oscillations usually present.

The application and limitations of this apparatus are the same as those of the effusion apparatuses already described in the literature.

ACKNOWLEDGMENTS

WADD TR 60-463 Pt I

REACTIONS OF TUNGSTEN AND MOLTEN ALUMINA

Charles L. Rosen, Alex A. Hasapis, Norman Sheppard, and James W. Wholley, Jr.

ABSTRACT

Molten alumina dissolves tungsten by intergranular attack to form a tungsten complex with a high disproportionation pressure.

The difference in alumina samples fused in tungsten crucibles in vacuum or in inert atmospheres can now be explained. The application of this reaction mechanism to Knudsen effusion and Langmuir evaporation experiments is pointed out.

I. INTRODUCTION

Previous reports have shown that molten alumina reacts with tungsten[1]. However, in view of the large number of investigations of this reaction that are still taking place, it was felt that a more complete interpretation of the reaction mechanism would be desirable.

The experiments which have been performed in order to elucidate the mechanism of the reaction involved melting charges of recrystallized alumina rods in a tungsten crucible in vacuum and in inert atmospheres.
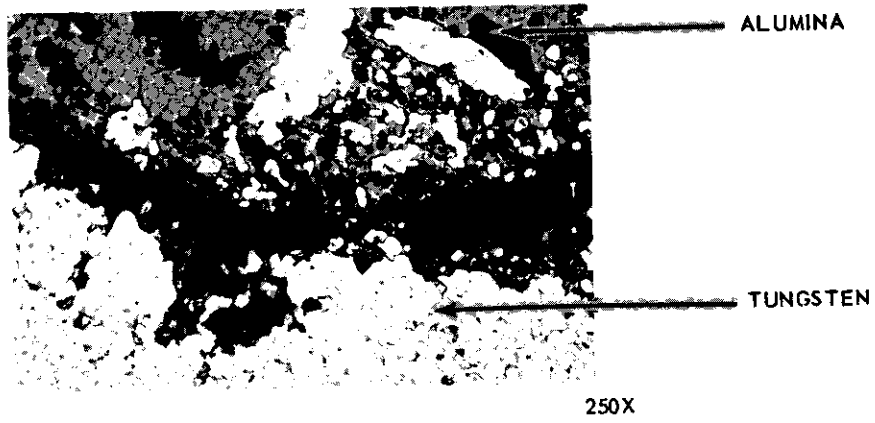
II. EXPERIMENTAL RESULTS

Metallographic examination of polished cross-sections of the crucibles have shown that alumina penetrates and attacks the tungsten at the grain boundaries (intergranular attack) as shown in Figure 1.

In all the experiments conducted in an inert atmosphere (A or He), a tungsten film forms over the liquid phase as shown in Figure 2. The film contains many hexagonal growth lamellae shown in Figure 3. X-ray and spectroscopic analysis have shown that the film consists only of tungsten metal. Below this film is a dark grey opaque form of alumina which when examined at room temperature by means of X-ray diffraction, consists of α-Al_2O_3, W, and three unidentified lines.
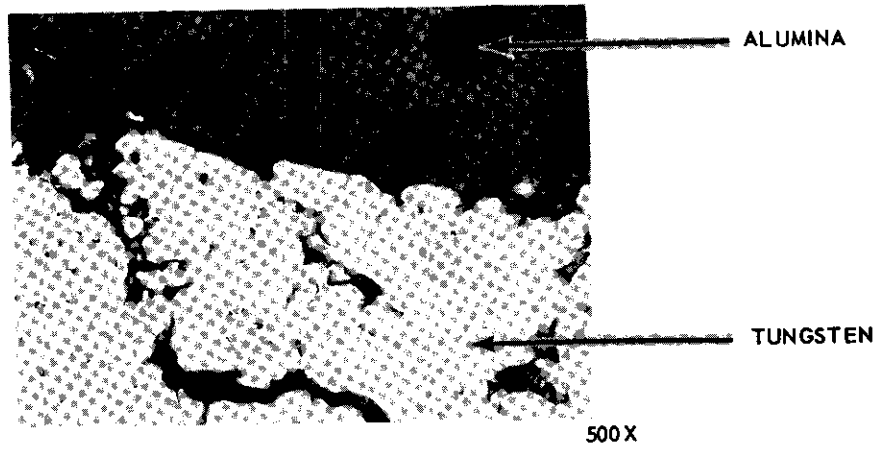
---

[1] Ackermann, R.J. and R.J. Thorn, J. Amer. Chem. Soc., **78**, 4169 (1959).
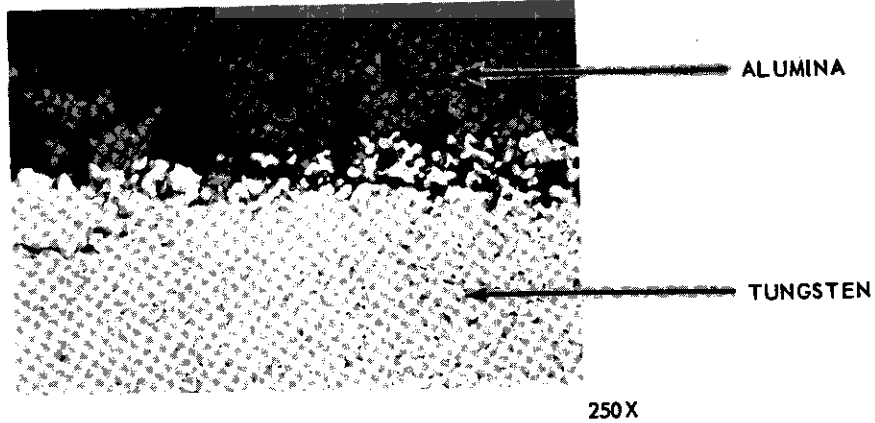
WADD TR. 60-463 Pt I

ALUMINA

TUNGSTEN

250 X

a. TUNGSTEN-ALUMINA INTERFACE

ALUMINA

TUNGSTEN
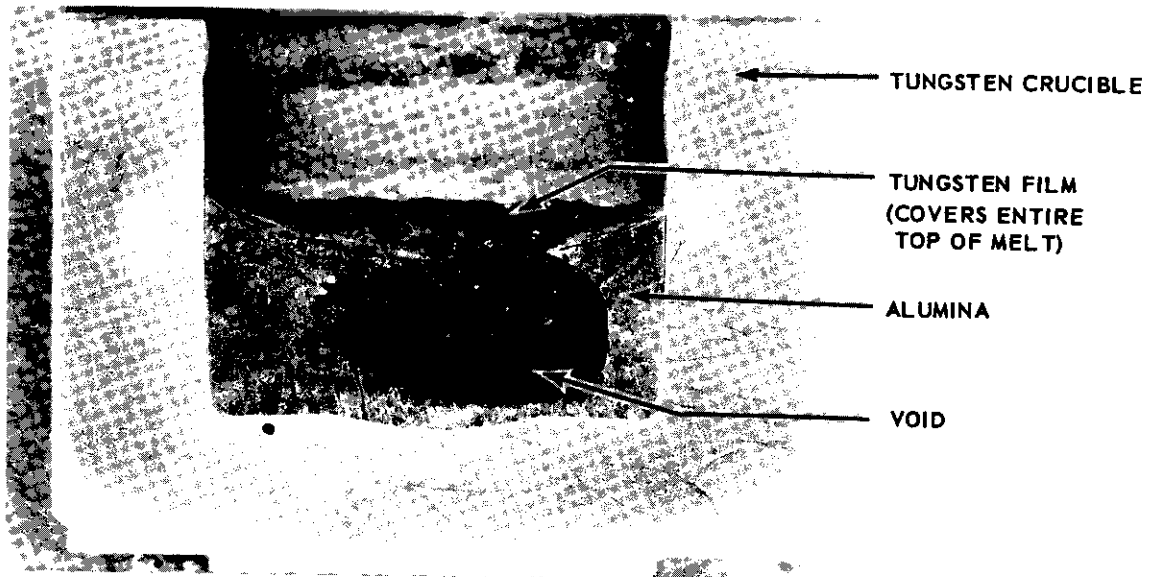
250 X

b. TUNGSTEN-ALUMINA INTERFACE

ALUMINA

TUNGSTEN

500 X

c. TUNGSTEN-ALUMINA INTERFACE
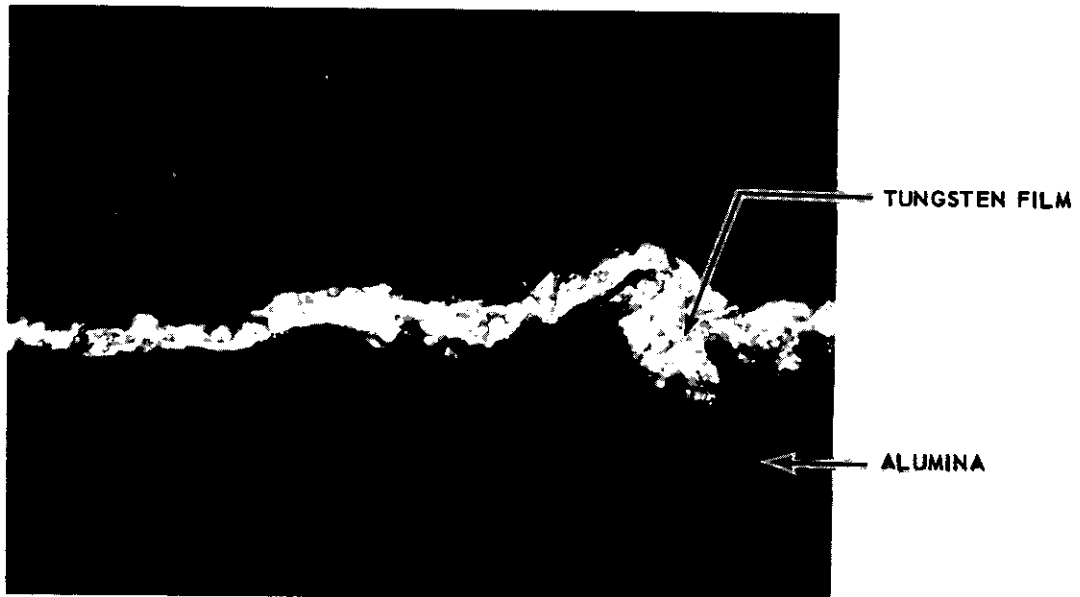
Figure 1 INTERGRANULAR ATTACK OF ALUMINA ON TUNGSTEN

WADD TR 60-463 PtI

-64-

TUNGSTEN CRUCIBLE

TUNGSTEN FILM
(COVERS ENTIRE
TOP OF MELT)

ALUMINA

VOID

4X

a.

TUNGSTEN FILM

ALUMINA

1000X

b.

Figure 2 TUNGSTEN FILM FROM ARGON EXPERIMENT

WADDTR 60-463 PtI

-65-

100X

Figure 3 TUNGSTEN GROWTH LAMELLAE

WADD TR 60-463 PtI

-66-

III. DISCUSSION OF RESULTS

In the experiments where alumina is fused in vacuum in a tungsten crucible without a lid, the tungsten film is not observed at the upper surface. However, a similar film is observed inside of any voids that occur in the vacuum melt and is observed on the top of the melt if a cover is placed on the crucible.

A plausible interpretation of the results is that the tungsten is dissolved by the intergranular attack of molten alumina, and that it goes into solution in some form other than tungsten. This tungsten bearing species is postulated to be in equilibrium with a vapor that readily disproportionates into tungsten metal (and some other constituent).

This reaction mechanism explains all the experimental results.

In vacuum where the mean free path is large, the tungsten bearing species and/or its decomposition products are carried away so that a tungsten film does not form at the surface.

In an inert atmosphere, in a covered crucible in vacuum, or inside a void where the mean free path is small, the tungsten is deposited on the melt surface where it precipitates in the form of hexagonal lamellae. These growth lamellae indicate that the film has been deposited from the vapor phase.

This reaction mechanism points out a possible source of error in the interpretation of Knudsen effusion and Langmuir evaporation experiments. In an open crucible, one may be measuring the rate of evaporation of the tungsten complex, whereas, in a closed crucible, where the molecules encounter collisions before leaving the crucible, the pressure may more nearly reflect the true vapor pressure of alumina. The placement and size of a Knudsen effusion orifice may lead to cases where one determines a pressure intermediate between the two extreme cases.

IV. ACKNOWLEDGMENTS

WADD TR 60-463 Pt I